2019-03

Performance analysis of standalone solar PV panel: case study of Arusha, Tanzania

John, Nickson

NM-AIST

https://doi.org/10.58694/20.500.12479/280

PERFORMANCE ANALYSIS OF STANDALONE SOLAR PV PANEL: CASE STUDY OF ARUSHA, TANZANIA

Nickson John

A Dissertation Submitted in Partial Fulfillment of the Requirements for the Degree of Master's in Sustainable Energy Science and Engineering of the Nelson Mandela African Institution of Science and Technology

Arusha, Tanzania

March, 2019

ABSTRACT

The purpose of this study was to carry out experimental and theoretical performance analysis of standalone solar Photovoltaic (PV) panel in tropical region. The study concentrated on the influence of poor PV panel positioning especially on the gap between the PV and roof, simulation, and over-shading. Three polycrystalline silicon panels of 100 watts each were selected from different manufacturers in local market. The panels were placed on a simple developed structure of corrugated metal sheet (CMS) roof; solar irradiance, gap between roof and PV panels, and temperature of the panels were the parameters affecting the PV system performance which were monitored. The monitored experimental parameters were used as the variable inputs for the Matlab simulation. In addition, foliage and opaque materials were used for outdoor shading experiments; the shading covered the area between ~3% and ~100% of the PV cells.

In the view of findings, the PVs' extra heat was originating from CMS roof vicinity. The highest temperature attained by the PV panel when it was directly mounted on the roof was 74.5 °C when the ambient temperature was 32 °C. The PVs' temperature dropped by ~5-9 °C while output power increased by ~5-11% when the gap enlarged from 0 to 50 cm at irradiance of 820 ± 10 Wm^{-2}. Experimental and simulated I-V curves were in good correlation hence validating the findings. Shading caused less energy harvested; the diminution depended on size of shaded cells and available irradiance; the results showed that even small shade can bring the system with no power generated. For common shading, the panels were able to generate a reasonable maximum power (111 to 136 watts) when shaded up to 22 % whilst slightest ranged between 5 watts to 22 watts when shading was 58% and above.

DECLARATION

I, Nickson John do hereby declare to the Senate of Nelson Mandela African Institution of Science and Technology that this dissertation is my own original work and that it has neither been submitted nor being concurrently submitted for degree award in any other institution.

…… **……**

Nickson John **Date**

The above declaration is confirmed

…….. **…….**

Dr. Thomas Kivevele **Date**

…… **……..**

Prof. Tatiana Pogrebnaya **Date**

COPYRIGHT

CERTIFICATION

The undersigned certifies that he/she has read and hereby recommend for acceptance by the Nelson Mandela African Institution of Science and Technology a dissertation entitled "Performance analysis of standalone solar PV panel: Case study of Arusha, Tanzania" in partial fulfillment of the requirement for the degree of Masters of Science in Sustainable Energy Science and Engineering of the Nelson Mandela African Institution of Science and Technology.

Principal Supervisor

Dr. Thomas Kivevele

Signature**: ……** Date**: …….**

Co-supervisor

Prof. Tatiana Pogrebnaya

Signature**: ……** Date**: ……**

ACKNOWLEDGEMENT

I am indebted to many people without whom this dissertation would still have been a distant dream. I acknowledge the invaluable contribution of every individual and institution for their contributions that led to the successful completion of this dissertation. Therefore, the list of contributors I humbly present here is by no means exhaustive.

First and foremost, my praise and thanks to God for the wisdom, strength and guidance to complete this study. I wish to express my sincere gratitude to Dr. Thomas Kivevele and Prof. Tatiana Pogrebnaya for their great, constructive, intelligent and professional expert feedback through the entire period of research study. They dedicated their time to help me all the time of my study in a friendly manner.

I also remember with affection my colleagues students of Science in Sustainable Energy Science and Engineering at the Nelson Mandela African Institution of Science and Technology. Special thanks to MEWES graduate seminar participants for the initiatives they took to ask questions that shaped my research progress.

My sincere thanks also go to all members of Electrical Engineering Department at Arusha Technical College (ATC) for their support in all stages of my research study. Last, but not least, I wish to thank my family in a very special way for their love, patience, care and perseverance especially when I was busy with my research works.

DEDICATION

This dissertation is dedicated to my colleagues, members of Electrical Engineering Department at Arusha Technical College (ATC) who struggled a lot to make my dreams of education came true. I also dedicate this dissertation to my family member for their support, prayers and encouragement towards all my educational endeavors.

TABLE OF CONTENT

ABSTRACT i

DECLARATION ii

COPYRIGHT iii

CERTIFICATION iv

ACKNOWLEDGEMENT v

DEDICATION vi

TABLE OF CONTENT vii

LIST OF TABLES x

LIST OF FIGURES xi

LIST OF APPENDICES xiii

LIST OF ABBREVIATION AND SYMBOLS xiv

CHAPTER ONE 1

INTRODUCTION 1

1.1 Background 1

1.2 Problem statement 3

1.3 Problem justification 4

1.4 Objectives 5

1.4.1 Main objective 5

1.4.2 Specific objectives 5

1.5 Research questions 5

1.6 Scope of research 5

1.7 Expected research outcome 6

CHAPTER TWO 7

LITERATURE REVIEW 7

2.1 Introduction 7

2.2 Solar photovoltaic generators 7

2.2.1 Solar PVs mounting 8

2.2.2 Effect of poor mounting of solar PV 9

2.2.3 Electrical characteristics of SPVP 11

2.3 Solar PV module simulation 12

2.4 Effects of shading on SPVP performance 14

CHAPTER THREE 15

MATERIALS AND METHODS 15

3.1 Introduction 15

3.2 Equipment / accessories and data acquisition system 15

3.3 Designing DAS circuit 17

3.4 Experimental setup 19

3.5 Experimental measurements 22

3.5.1 Irradiance variation during the test days 22

3.5.2 Impact of CMS on PV panel performance 22

3.5.3 Effect of variance in gap on PV performance 24

3.5.4 SPVP Matlab simulation 25

3.5.5 Effect of partial shading on SPVPs 27

CHAPTER FOUR 29

RESULTS AND DISCUSSION 29

4.1 Introduction 29

4.2 Irradiance variation during the test days 29

4.3 Impact of solar irradiance and CMS roof on PV panel performance 32

4.4 Effect of variance in gap between CMS roof and panel on PV performance 38

4.5 Solar PV panels Matlab simulation 44

4.6 Effect of partial shading 48

CHAPTER FIVE 53

CONCLUSION AND RECOMMENDATIONS 53

5.1 Summary of the study 53

5.2 Conclusion 53

5.3 Recommendations 54

REFERENCES 56

APPENDICES 63

OUTPUTS 75

Output 1: Acceptance letter for paper publication 75

Output 2: Research poster 76

LIST OF TABLES

Table 1: Equipment and accessories 16
Table 2: Electrical characteristics of the three solar panels at STC 20
Table 3: Thermal characteristics of the three solar panels at STC 21
Table 4: Mechanical design characteristics of the three solar panels 21

LIST OF FIGURES

Figure 1: Solar PVs mounted with different PV-roof spacing 3
Figure 2: Different roof pitches with dissimilar mounted SPVP on structures in same geographical area 8
Figure 3: Solar PV cell equivalent circuit 12
Figure 4: Clad board layout components connections 18
Figure 5: Clad board circuit with soldered components connections 19
Figure 6: Experimental setup 20
Figure 7: Solar PVs mounted on panel holder at 0 cm from CMS 23
Figure 8: Circuit diagram for I-V curves measurements 24
Figure 9: I-V experimental data collection 24
Figure 10: Comparison of readings from two solar meters, TES 132 USB and volt-craft PL-110SM 30
Figure 11: Irradiance at different test days 31
Figure 12: Variation of Ta and Rh versus irradiance 31
Figure 13: Variations of temperatures versus time of a day 33
Figure 14: Temperature distribution over the system with the panel B mounted directly on the roof 34
Figure 15: Panels' temperature variation versus irradiance 35
Figure 16: Short circuit currents for three solar panels versus irradiance for h = 0 37
Figure 17: Open circuit voltages for three solar panels versus irradiance for h = 0 37
Figure 18: I-V curves for three solar panels at different irradiance for h = 0 38
Figure 19: Variation of maximum power versus irradiance for h = 0 38
Figure 20: Temperature variation depending on gap alteration from h=0 -50 cm at G=820±10 Wm^{-2} 39
Figure 21: Short circuit current and currents at maximum power for 0-50 cm gap alteration at G=820±10 Wm^{-2} 41
Figure 22: Open circuit voltages for 0-50 cm gap alteration at G=820±10 Wm^{-2} 41
Figure 23: I-V curves at h=0 and50cm at G=820±10 Wm^{-2} 42
Figure 24: Maximum power solar panels performance for 0 cm-50 cm PV CMS gap alteration at G=820±10 Wm^{-2} 42
Figure 25: Impact of a gap h between the solar panels and roof on the panels' performance (efficiency) measured outdoor at solar irradiance 820±10 Wm^{-2} 43

Figure 26: Comparison of panels' fill factors at solar irradiance 820±10 Wm^{-2} and at STC 43
Figure 27: Simulated I-V curves at different irradiance and panel's temperature 46
Figure 28: Simulated I-V curves at different irradiance and panel's temperature 47
Figure 29: Simulated and experimental I-V curves at G=820±10 Wm^{-2} 47
Figure 30: Effect of common shading on short circuit currents for G= 930±50 Wm^{-2} at h=50 cm 49
Figure 31: Effect of common shading on open circuit voltage for G=930±50 Wm^{-2} at h=50 cm 50
Figure 32: Effect of uncommon shading on short circuit current at 400±10 Wm^{-2} at h=50cm .51

LIST OF APPENDICES

Appendix 1: Data acquisition system input codes …….…….……63

Appendix 2: Panel holder stand …….…….....69

Appendix 3: Bottom panel stand ……..…….……70

Appendix 4: Corrugated metal sheet roof holder …….……..71

Appendix 5: Experimental mounting structure …….…… ……..72

Appendix 6: Code function for I-V curve …….……... ……..73

Appendix 7: Command code for solar irradiance …….……..74

LIST OF ABBREVIATION AND SYMBOLS

CMS	corrugated metal sheet
DAS	data acquisition system
h	gap size between the solar PV panel and the roof
I_A, I_B, I_C	short circuit currents for panels A, B, and C
NOCT	nominal operating cell temperature
PV	photovoltaic
SPVP	solar photovoltaic panel
STC	standard test condition
T_A, T_B, T_C	rear surface panel temperature for panels A, B, and C
T_a	ambient temperature
T_b, T_c,T_t,	bottom, center and top rear side panel temperature of the same panel
T_g	temperature of the gap between PV and CMS roof
T_S	temperature of the front surface of CMS
V_A, V_B, V_C	open circuit voltage for panels A, B, and C

CHAPTER ONE

INTRODUCTION

This chapter provides introductory information about the background of the study, statement of the problem, problem justification, purpose of the study, research question, scope of research, and significance of the study.

1.1 Background

Energy is among essential factors for social, economic and industrial development. Despite of its negative impacts on the environment, fossil fuel is still highly used for energy production. It is obligatory for countries to inquire for environmental friendly alternatives energy sources that are renewable to encounter the growing energy demand (Sheya and Mushi, 2000). Renewable energy covers all energies occurring naturally in the environment and capable of being replaced by natural processes. At present, the most available and useful renewable energy sources worldwide are those delivered through hydropower, biomass, solar, geothermal, wind, ocean tidal and wave (Demirbas, 2005; Jacobson, 2007; Panwar *et al*., 2011 Deichmann *et al*., 2011; Ellabban and Blaabjerg, 2014). Solar energy is one of the paramount renewable energy sources with minimum negative effects on the environment (Solangi *et al*., 2011). It is a resource that reaches the earth as sunlight that exists worldwide compared to other energy resources which are site specific. Sunlight is collected and converted into electricity directly by photovoltaic (PV) cell technology (Parida *et al*., 2011; Khare *et al*., 2013; Kulworawanichpong and Mwambeleko, 2015). Hence using electricity produced by solar PV system in domestic applications, particularly in places which receive plentiful solar irradiance like Tanzania, is one of the best solution for rural electrification (Mellit *et al*., 2008; Szabo´ *et al*., 2011; Kihwele *et al*., 2012; Ondraczek, 2013; Ahlborg and Hammar, 2014; Nyari *et al*., 2015).

The performance of solar PV panel (SPVP) is influenced by excessive temperature on cells. Outdoor roof mounted SPVPs' temperature varies depending on air temperature, level of direct sunlight, and roofing material (Honsberg and Bowden, 2014; Honsberg and Bowden, 2016). The increase in PVs' temperature lowers the efficiency of PVs (Fesharaki *et al*., 2011; Dubey *et al.*, 2013) and it decreases the life span of the whole PV modules. The

impact of increasing temperature on solar cell are exposed by the electrical characteristic curve (Fesharaki *et al*., 2011; Tyagi *et al*., 2013; Kaldellis *et al*., 2014; Chander *et al*., 2015).

Several studies have been done to evaluate the performance of solar PVs and most of them were site specific. Mattei *et al*. (2006) reported the influence of ambient temperature, solar irradiance, and wind speed affected the PVs' output. Fesharaki *et al*. (2011) performed a simulation study on the effect of temperature on PV cell efficiency under cloudy and sunny conditions. They pointed out that with increasing time, the efficiency decrease with temperature increase and vary with temperature and sun radiation. Khan *et al*. (2017) found that power decreased due to high operating temperatures under the same solar radiation conditions and with decreasing solar radiation. Ramabadran and Mathur (2009) reported that power dissipation in the SPVP might be significant primarily to the rise in its temperature which leads in producing hot spot. These phenomena can harm the panel's encapsulation and ultimately module failure will occur. Fialho *et al*. (2014) did a theoretical and experimental on two monocrystalline PV panels technology connected in series. The study shaded only one-whole SPVP. The result showed that there was some distortion in I-V simulated curve. The efficiency of SPVP as revealed in previous studies depends on numerous technical, geographical and environmental factors. Less solar irradiance reaching the cell, high PV's temperature, less relative humidity, improper mounting, poor module orientation, and shadowing are the factors reported to affect module power output (Meral and Diner, 2011; Mekhilef *et al*., 2012; Sharma and Chandel, 2013; Chikate and Sadawarte, 2015; Elminir *et al*., 2006; Ramabadran and Mathur, 2009; Tyagi *et al*., 2013; Darwish *et al*., 2013).

Despite the fact that a significant number of studies have reported performance of PV panels but none of them has quantified outdoor experimental performance of standalone SPVPs in terms of the influence of PV – corrugated metal sheet (CMS) roof gap (Fig. 1). Therefore, the aim of this study was to investigate and analyse outdoor performance of polycrystalline silicon solar panel mounted on sloped corrugated metal sheet roof. The study was done on polycrystalline PV panels of the same size from three different manufacturers to observe if there were significant differences in terms of performance when they were mounted on outdoor pitched CMS roof. The investigation was done by varying the gap between roof pitch and the PV panel, and the influence of common and uncommon panel shading. In all experiments, three PV panels from different manufacturers used were named as panel A, B

and C and kept on the same environmental conditions. Assessing the outdoor performance of SPVPs for a particular application is the best practice in order to identify ways to increase panels' output and decreasing panels' degradation or destructive impacts when they are installed in real working environment.

Figure 1: Solar PVs mounted with different PV-roof spacing

1.2 Problem statement

The main task in using a SPVP generator is to wrestle its nonlinear output parameters, which change with its temperature and irradiance. Along with truthfulness that SPVPs do not pollute the environment when they are in use; yet they have some drawbacks to its outputs when they are exposed to excessive temperature and when the front surface is subjected to shadow situations. The increase of SPVP's temperature and shadowing accumulation on front surface decreases its performance (Touati *et al*., 2012; Dubey *et al*., 2013). Usually solar PV modules are tested for power output at 25 °C, that if a panel temperature coefficient rating is -0.5% per °C, the output power of the panel will decrease by a half percent for each degree the temperature rises above 25 °C (Mattei *et al*., 2006; Grubišić-Čabo *et al*., 2016).

Most of remote rural roof mounted PVs are done according to the roof pitch structure whilst gaps and tilt angle are not much observed. It has been witnessed that some of SPVPs are placed directly on or near the CMS roof whilst natural air flow between the PV and the roof be blocked. Though it is recommended to mount panels on structure above CMS roof, it has

not clear what is the best gap between PV mounting structure and the available different pitched CMS roof. This situation has led to have various PV mounted structures on pitched CMS roof while others are being installed directly on it as depicted in Fig. 1. This kind of mounting can cause the panel to suffer from hotness and may affect the performance. Generally, there is no uniformity in mounting the solar PV panel on the roof especially in the same geographical area (Fig. 1). The output of the SPVP would be increased by optimizing the tilt angle and PV- roof ventilation gap (Gooding *et al*., 2015; Stathopoulos, 2003).

A non-uniform insolation such as partially shaded creates more complicated output characteristics resulting in multiple peaks (Patel and Agarwal, 2008). Hot spot occurs when individual cells are partially shaded which causes enormous power dissipation ensuing in local over heating which in turn lead to destructive effects, such as cells or glass cracking, melting of solder or degradation of the solar cell (Ramabadran and Mathur, 2009). Dust and solid particles varying in type, composition and shape scatters sun's radiation so that it cannot reach the cell (Elminir *et al*., 2006; Mani and Pillai, 2010; Darwish *et al*., 2013). It is clearly seen from Fig. 1 that the dust are deposited on SPVP. However, it is very important to understand the outdoor mounted SPVP characteristics under all conditions in order to use them effectively. Thus this study aims to address the spacing between the pitched CMS roof and the solar PV using three panels from different manufacturers, and effect of shading, a study is conducted in Arusha, Tanzania.

1.3 Problem justification

Due to high increase in energy demand for society economical activities, maximization of using the advantage of solar energy is of vital importance. Keeping in mind that it takes direct photon on the surface of the PV to produce the maximum-rated power, the conditions such as temperature, shadows, improper mounting and orientation will reduce the actual solar panel outputs. Cooling the SPVP temperature and being it clean all the time will enable a better utilization of solar energy and it would lead to growth in economic and social activities.

Active cooling and passive cooling are techniques have been used for cooling SPVPs. Active cooling requires a separate system which will remove heat while passive cooling techniques use natural conduction to enable heat extraction. The assembly and maintenance

of the active cooling system are expensive and there is a possibility that the system maintenance cost could outweigh the benefits of the improved electrical yield as compared to natural air passive cooling. Hence, findings of PV-CMS gap on a roof and utilizing a passive air cooling would be helpful for energetic and economic efficacy of the solar system.

1.4 Objectives

1.4.1 Main objective

The main objective of this study was to carry out experimental and theoretical performance analysis of standalone solar PV panels (polycrystalline) from three different manufacturers: Case study in Arusha, Tanzania.

1.4.2 Specific objectives

The main objective of the study was achieved by pursuing the following specific objectives:

i. To evaluate the performance of standalone SPVP on natural air passive cooling by varying gap between pitch CMS roof and panel.
ii. To assess the simulation performance of standalone SPVP under real working conditions and compare to experimental results.
iii. To assess the effects of shading on performance of SPVPs.

1.5 Research questions

i. What is the impact of a panel-roof gap alteration on the panel performance?
ii. How do simulated and experimental performances of the SPVP differ?
iii. To what extent does shading affects the SPVP output parameters?

1.6 Scope of research

This study focused on experimental and theoretical performance analysis of standalone solar PV panel (polycrystalline) from three different manufacturers, case study in Arusha, Tanzania. It was confined to evaluate the performance of standalone SPVP on natural air passive cooling by varying gap between pitch CMS roof and panel, to assess the theoretical performance of standalone SPVP under working conditions as well as to assess the effects of shading on performance of SPVPs.

It was conducted during the academic year 2017/2018 at NM-AIST. The experimental work on research was localized and set at NM-AIST main campus and only one experimental point was set.

1.7 Expected research outcome

Power from solar has proven driver of economic development, hence, production activities will be increased due to availability of assured power. The study outcome enhances the standalone PVs outputs, and operating time due to avoidance of cracking caused by heat dissipation in shaded cell. Replacement of worn out system components caused by losses from the SPVP will be minimized. The study enhances awareness to system owners and the community in general the effect of improper installed SPVPs as well as system maintenance.

CHAPTER TWO

LITERATURE REVIEW

2.1 Introduction

This chapter is about the review of literature related to the research topic about photovoltaic generator, mounting of SPVPs, effect of poor mounting of solar PVs, electrical characteristics of PV, simulation and effect of shading.

2.2 Solar photovoltaic generators

SPVPs are built up with combined series/parallel combinations of solar cell electrically connected together (Kulworawanichpong and Mwambeleko, 2015). The panel is then sealed and covered with a non reflective glass but ensuring sunlight can still reach the cell. The configuration is then placed in unbending metallic frame.

All SPVP converts the incident solar radiation into electricity (direct current) directly without noise and polluting (Darwish *et al*., 2013). They are sensitive to temperature; greater PV cell temperature is among of the parameters that affect the performance of the SPVP causing deviation from STC. Solar radiation that has been absorbed but not being converted to electricity is converted to heat energy which in turn decreases the efficiency of the SPVP. On roof mounted SPVP, its temperature varies depending on air temperature, level of direct sunlight, and roofing material. The major impacts of increased SPVPs' temperature on performance are reduced its output voltage, lowered output power and the efficiency drops significantly with the rise of panel temperature (Fesharaki *et al.*, 2011; Dubey *et al*., 2013). A daily PVs' temperature increase; decreases the span life of the whole PV modules. Much power will be lost hence operation and maintenance cost will be raised.

Placing the SPVP directly on or near CMS (Fig. 2) can make the panel to be subjected to conduction, radiation and convection heat absorption. Thermal energy on a SPVP can be moderately avoided by applying a suitable method of thermal extraction. Natural air circulation is among methods for cooling SPVP. Usually SPVP are tested for power output at 25 °C; if a panel temperature coefficient rating is -0.5% per °C, the output power of the panel will decrease by a half percent for each degree the temperature rises above 25 °C. The impact of increasing temperature on solar cell is shown by the I-V characteristic curve (Fesharaki *et al*., 2011); Tyagi *et al*., 2013; Kaldellis *et al*., 2014; Chander *et al*., 2015). The

open-circuit voltage decreases with increase in temperature while short-circuit current increases slightly with temperature increase. The increase in short circuit current rises power dissipation in the module which is regarded as a loss hence results in reduced PV output power.

Figure 2: Different roof pitches with dissimilar mounted SPVP on structures in same geographical area

2.2.1 Solar PVs mounting

SPVPs are mounted on a structure at a fixed tilt angle facing sun's path. The tilt angle can either be facing south for those who are in the northern hemisphere or facing north for those who are in the southern hemisphere. The best inclination angle determination of SPVP is important to its effective operation since improper setting leads to loss of solar power harvesting. The optimal inclination angle determination is centered on maximizing the solar insolation hitting on a sloped surface and it is usually a site specific (Yadav and Chandel, 2013; Jacobson and Jadhav, 2018). The structure can be either non-tracking, manually tracking or automatic tracking structure that tracks the sun permitting them to capture more

sunlight. Solar tracking is a great way of increasing the output power from the SPVP. It rotates the panel or array so that they always directly face the sun's rays.

In Tanzania; rural individuals' domestic standalone SPVPs mounting are done on the top of pitched CMS roof which are non-rotating structures. Mounting SPVP on pitched CMS roof is challenging due exposing to weathering elements, including heavy winds and large temperature gradients. For maximum output, SPVP must be installed perpendicular to the sun's rays though it is generally useful and common for roof-top installations to follow the roof pitch and orientation. Poor mounting of a SPVP can lead to extremely inefficient panels that do not provide a great amount of power for your need. Structural elements of the panels tend to accumulate heat when exposed to sunlight and this may degrade the performance as their temperature increases. Building owners have different selections of pitching their roofs according to geographical area (Bergamasco and Asinari, 2011). While some opt for hip roofs or gable roofs with either highly raised roofs or for low ones others settle flat roofs depending on what they want to achieve in their home but also roof shape considers the wind pressures on roofs. Since there are many pitch roofing styles and different kinds of roofing materials, there is no general minimum roof pitch around the world. The output of the SPVP would be increased by optimizing the tilt angle and PV- roof ventilation gap (Gooding *et al.*, 2015; Stathopoulos, 2003). It is still challenging to install on a high roof pitch; as most of the installed PVs in Tanzania are done according to the roof pitch while others air flow being blocked on one side.

2.2.2 Effect of poor mounting of solar PV

The operating temperature of a module is determined by the equipoise between the heat of the SPVP, the heat lost to the environment and the ambient operating temperature. The heat produced by the module depends on the operating point of the module, the solar cells optical properties, encapsulation quality and the packing of the solar cells in the SPVP. High SPVPs' temperatures increase stresses associated with thermal expansion and also increase panels' degradation. Poor encapsulation of solar cells into a SPVP may alter the heat flow into and out of the SPVP, thereby increasing the operating temperature of the SPVP hence reducing its voltage and the output power. The heat lost to the environment can spread out through radiation, conduction, and convection. These loss mechanisms depend on the thermal resistance of the module materials, the emissive properties of the SPVP, the ambient conditions and wind speed in which the module is mounted. If not properly mounted; SPVPs

may be affected by conduction, radiation and convection heat transfer (Honsberg and Bowden, 2014).

Conductive hotness losses are retained to thermal pitches among the SPVP and other constituents including the nearby air with which the SPVP is in contact. The capacity of the SPVP to transfer heat to its surroundings is categorized by the thermal opposition and alignment of the things used to encapsulate the solar cells. The temperature variance is the dynamic strength overdue the conductive stream of heat in a physical with a set thermal opposition. The thermal opposition of the SPVP is influenced by the coverage of the material and its thermal conductivity. The thermal resistance of the front and rear surfaces of the SPVP would add in series. Assuming that materials used are identical and are in steady state, heat generated by the SPVP is given by the product of change in temperature between the two materials, area of the surface conducting heat, and the thermal conductivity divided by the length of the material through which heat must travel (Equation 2.1). It is evident that if the length (gap) between the materials is very small, heat generated by the SPVP will be high. Hence PVs pinned directly to the pitched CMS roof will always suffer from heat.

$$H = \frac{\Delta T \times A \times k}{L} \tag{2.1}$$

where: H is the heat generated by the solar PV module, ΔT is the change in temperature between the two materials in °C, A is the area of the surface conducting heat, L is the length of the material through which heat must travel; and k is the thermal conductivity in units of W m^{-2} $°C^{-1}$ (Honsberg and Bowden, 2016).

Convective hotness transfer ascends from the passage of heat away from a surface as the consequence of one physical touching transversely the surface of another. Blowing wind supports the heat transfer in along the SPVP surfaces. Convective heat transfer in SPVPs is the product of convection hotness transfer, change in temperature between the two materials, and area of the surface conducting heat (Equation 2.2).

$$H = A \times \Delta T \times h \tag{2.2}$$

where: h is the coefficient of convection hotness transfer in units of W m^{-2} $°C^{-1}$ other parameters are as stated above (Honsberg and Bowden, 2016).

Again; heat energy from sun reaches the SPVP and the surrounding environment through radiation. Surrounding object emits radiation to the SPVP based on its temperature (Honsberg and Bowden, 2016). It should be noted that the temperature of CMS roof may reach as high such that when the SPVP is directly laid on CMS roof, it will continue to get heat through conduction hence reducing the performance and efficiency.

2.2.3 Electrical characteristics of SPVP

The SPVP output voltage is a function of the photocurrent that mainly determined by load current depending on the incident solar radiation level during the operation. The I-V characteristics curves are nonlinear which they vary with PV cell temperature and solar irradiation. The fundamental parameters related to solar PV panel characteristics are short circuit current and open circuit voltage. The output of the current source is directly correlated to the light falling on the cell. The solar cell it produces neither a current nor voltage during darkness.

The electrical characteristics of a SPVP can be represented graphically summarizing the relationship between current and voltage or power and voltage produced on a typical solar panel at the referenced conditions of irradiance and temperature. Solar PV panel electrical characteristics can be obtained either through laboratory work, outdoor experiment or simulation software. Solar PV panel output are rated by manufacturers under standard test conditions (Elminir *et al.*, 2006; Fesharaki *et al.*, 2011; Tyagi *et al.*, 2013). Manufacturer's specifications usually are the fixed initial input data used as a reference, however, the variable input data are to be considered according to available (present) climate parameters.

Plotting electrical characteristic curves of the SPVP cells for a certain working irradiance and certain SPVP cell temperature, among them one should fixed (Ishaque *et al*., 2011). The performance testing conditions are sensibly controlled in laboratory but in actual outdoor mounting the situation is not similar from one geographical area to another. Mattei *et al*. (2006), Fesharaki *et al*. (2011) and Dubey *et al*. (2013) explored the equation for the effect of temperature on solar PV efficiency (Equations 2.3 and 2.4). It is clear from the expression that; higher panel temperature lowers the efficiency of the SPVP. Again, Chander *et al*. (2015) reported that the efficiency of a SPVP can be obtained from a fundamental equation but through laboratory work. Basing on the development and analysis of models that are

representative regarding the real system and the goals of the study it is possible to obtain scientific support for the decision making based on electrical characteristics of the study.

$$\eta c = \eta Tref[1 - \beta ref(Tc - Tref) + \gamma \log_{10} I(t)] \quad (2.3)$$

$$\text{and} \quad Tc = Ta + (NOCT - 25\ ^{\circ}C)\frac{G}{1000} \quad (2.4)$$

where η_{Tref} is the panel's electrical efficiency at reference temperature T_{ref}, and at solar radiation of 1000 Wm^{-2}, γ_{ref} is the solar radiation coefficient, and β_{ref} is the temperature coefficient. T_c is the cell temperature, *Ta* is the ambient temperature of 25 °C at AM 1.5, NOCT is the nominal operating cell temperature and *G* is the measured solar radiation.

2.3 Solar PV module simulation

Simulation is a depiction of the operational system or generalized of reality. They consciously highlight one part of veracity at the expenditure of other parts. It is done focusing the important aspect of the attention simulation. Through simulation, a prototype can be made with unrestricted dissimilarity, producing various results which can be presented either in computation of numeric data, creating graphics for scientific use, modelling and simulating data, and analysing data. These proficiencies allow analysis and thoughtful of how distinct components interact and affect the simulated setting. Basing on the development and analysis of models that are representative regarding the real system and the goals of the study it is possible to obtain scientific support for the decision making based on electrical characteristics of the study.

Solar PV panels are normally represented by a simplified equivalent circuit model (Fig. 3). Understanding the physical arrangement of the elements of the PV cell as well as the electrical characteristics of each element enables to develop an accurate equivalent circuit expressions for a PV cell (Fara and Craciunescu, 2017).

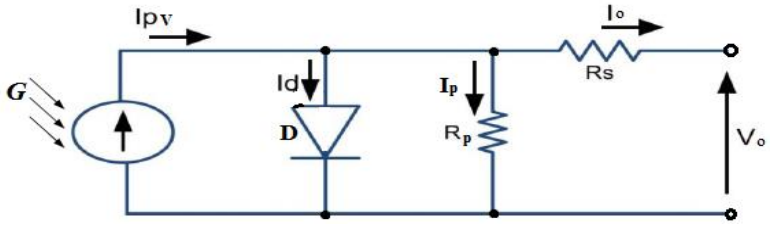

Figure 3: Solar PV cell equivalent circuit

The I_{PV} is the current generated by the incident light and it is directly proportional to the sun irradiation G, Id is the diode saturation current, I_0 is the output (load) current. R_S is the equivalent series resistance of the panel and R_P is the equivalent parallel resistance. Practical panel is composed of several electrically connected (series/parallel) PV cells (Sharma and Chandel, 2013). SPVP cells connected in series provide greater output voltages whereas cells connected in parallel increase the current. The observation of the characteristics at the terminals of the PV panel requires the inclusion of additional parameters to the basic equation that could be developed from Fig. 3. More sophisticated models that present better accuracy have been proposed by some authors and serve for different purposes. In and study, for easiness the single diode model of Fig. 3 is considered in this study though an extra diode was used to represent the effect of the recombination of carriers (Ishaque *et al*., 2011; Bonkoungou *et al*., 2013). This circuit suggest an upright cooperation between simplicity and accuracy and has been used in several previous works (Tsai *et al*., 2008; Bellia *et al*., 2014; Park *et al*., 2014).

Manufacturers of SPVP, usually provide only a few experimental data about thermal and electrical characteristics. Appropriate certain parameters required for correcting SPVP models cannot be found in the manufacturers' data sheets. These include the light generated currents, the series and shunt resistances, the diode ideality constant, the diode reverse saturation current, and the band gap energy of the semiconductor. The information that the SPVP data sheets bring basically are: short circuit current, open circuit voltage, the current at the maximum power point, the voltage at the maximum power point, the short circuit current/temperature coefficient, the open circuit voltage/temperature coefficient, and the maximum experimental peak output power. These informations are always provided with reference to the standard test conditions (STC) of temperature and solar irradiation of 25 °C, 1000 Wm^{-2} and Air Mass of 1.5. Some manufacturers provide I-V curves for numerous solar irradiance and panel temperature.

The I-V curves of the SPVP depend on the interior features like R_S, R_P and on external impacts such as temperature PV cells and solar irradiance level. The amount of irradiance affects the generation of charge carriers and therefore the current produced by the panel. The assumption light-generated current equal to short circuit current is generally used in photovoltaic models because in practical panel the series resistance is low and the parallel resistance is high. Generally, the light generated current of the photovoltaic cell depends

linearly on the solar irradiance and similarly is influenced by the temperature (Salmi *et al*., 2012; Tsai *et al*., 2008; Meral and Diner, 2011; Sharma and Chandel, 2013).

2.4 Effects of shading on SPVP performance

Solar intensity reaching SPVP varies time to time of a day. These variations practically affect the output parameters. Assuming a clear sky; irradiance received by solar cell is affected by dirt accumulation and shadow on the front surface of the SPVP. Shading blocks sunshine from penetrating the glass and exciting the electrons underneath. Shading reduces the energy input to the solar PV system and also increases the losses in the system. It can occur when fixed or moving object be in between the solar irradiance and the front surface of SPVP. Shading can be partial cell, partial SPVP or full module. Shadowing of the fixed objects like tree, building, or leaves on the front surface of the SPVP affects light intensity incident reaching the solar cell. Shading SPVP can reduce the power output to zero.

Generally, when the part of a PV panel is shaded, shaded cells cannot produce as much short circuit current as compared to those which are not shaded. Meanwhile PV cells are usually connected in series in a panel; the similar quantity of short circuit current must flow through every cell. Unshaded cells will force shaded cells to pass more short circuit current than their new short circuit current. The only tactic that shaded cells can run at a current greater than their short circuit current is to work in the region of negative voltage there by causing a net voltage loss in the system. Shaded cells begin to absorb power hence acting as a load dissipating power as heat causing hot spots (Karatepe *et al*., 2007).

Several studies worldwide have been done on shading but none of them did experimentally for SPVP from different manufactures with common and uncommon shading. This study was aimed to study experimentally how partial shading affects outputs. Analysing the partial shading can help in decision-making in selecting the panel, increases energy harvested and decreases panel’s destructive impacts.

CHAPTER THREE

MATERIALS AND METHODS

3.1 Introduction

This chapter focuses on the methodology that was employed in the research about the experimental and theoretical performance analysis of standalone solar PV panels. This chapter describes in details equipment / accessories and data acquisition system (DAS), designing of DAS, experimental setup, experimental measurements: irradiance variation during the test days, impact of CMS on PV panel performance, effect of variance in gap on PV performance, Matlab simulation, and effect of partial shading.

3.2 Equipment / accessories and data acquisition system

The experiment was setup on a simple developed platform structures serving as house roof as depicted in Fig. 6. Photovoltaic mounting structure was made of square mild steel hollow section, roofing was made of two CMS with three meters length each locally known as "Imara Kiboko AL-ZN gauge 30 AZ-85" to a 30×30×2 mm mild steel hollow section. Panel holder was made of 30×30×2 mm mild steel hollow section whilst bottom panel stand was made of 40×40×2 mm mild steel hollow section. Equipment and accessories used in the research and their functions are summarized in Table 1 as also viewed in Fig. 6.

Table 1: Equipment and accessories

Name	Description	Function
A, B, C	Panel A, panel B, panel C	Conversion of solar irradiance to electricity
MS	Mounting structure	Support for solar PV panels
CMS	Corrugated metal sheet roof 20° pitched	Support for solar PV panels
DAS	Data acquisition system	Measurement and recording of parameters under study
Ts	Temperature sensor	CMS front surface temperature measurement
T_g	Temperature sensor	PV-CMS gap temperature measurement
T_A, T_B, T_C	Temperature sensors	Panel A, B, and C temperature measurement
T_t, T_c, T_b	Temperature sensors	Temperature measurement at the top, center, bottom of panel B
DHT	Digital humidity temperature	Measurements of ambient temperature Ta and relative humidity Rh
SSN 22e	USB data logger	
TES	USB Solar power meter	Measurement of solar data logging
K	Kestrel	Wind speed measurement

Data acquisition system (DAS) was designed and made to read and record required parameters of the study. The device was made using single sided copper clad board, mega Arduino development board, liquid crystal display (LCD) 20 columns by 4 rows, switching transistor (Q), diodes (D), resistors (R), relays (RL), digital humidity-temperature (DHT)-22 sensor, linear monolithic (LM35) sensors, real time clock (DS1307), secure digital (SD) card and card reader (MMC), voltage sensor (0.25 W carbon film resistor arranged in potential divider) and ACS712-30A current sensor as shown in Fig. 4. Proteus and Arduino technologies were used in achieving the designing the circuit for electrical and electronic components connections whilst C language was used to program the circuit as depicted in Appendix 1. Electronic components were inserted in drilled holes through appropriate electric circuit connections and were soldered to make good contacts according circuit of Fig. 5. The circuit was powered by a 9 V battery. Calibrations were made and configured using other already manufactured devices measuring the same parameters. The SSN-22e was

used for temperature and relative humidity. The Gw Instek GDM-396 multimeter and Fluke 117 multimeter were used for measurement of current and voltage respectively.

3.3 Designing DAS circuit

A single sided copper clad board is a board that one side is coated with copper material. It is used electrically to interconnect electronic components found in electronic devices like radios, televisions, remote control and other alike that form a circuit. Usually a thin layer of conducting material (substrate) is printed on the surface of an insulating board where individual electronic components are inserted in a drilled hole on the surface of the substrate and soldered to the interconnecting circuits.

Electrical connections between the circuit components were achieved by designing the circuit using Proteus software. The circuit was printed on a glossy paper using powder ink. The printed circuit was then folded on copper coated side of a clad board after cleaning using steel wool. The side was then ironed for seven minutes with high heat. The clad board and the attached glossy paper was immediately dropped in room temperature water and left for two minutes for detaching it from the clad board. After removing a glossy paper, circuit lines on a copper side clad board was drawn; the circuit that drawn on the glossy paper was transferred to the copper sided clad board. The clad board was then dropped in a mixture of ferric chloride and hot water; leaving it for five minutes purposely for removing all unwanted copper substrate from the circuit. The circuit lines (contaminated powder ink) were then cleaned using steel wool leaving a conducting part of the circuit. The terminals of each circuit line were drilled using a one millimetre diameter drill bit. Electronic components were inserted in drilled holes through appropriate locations and then were soldered to make good contacts as shown in Fig. 5. The circuit was fixed in housing. Input function codes were written (Appendix 1) and fed into DAS to enable device to interpret the measured parameters.

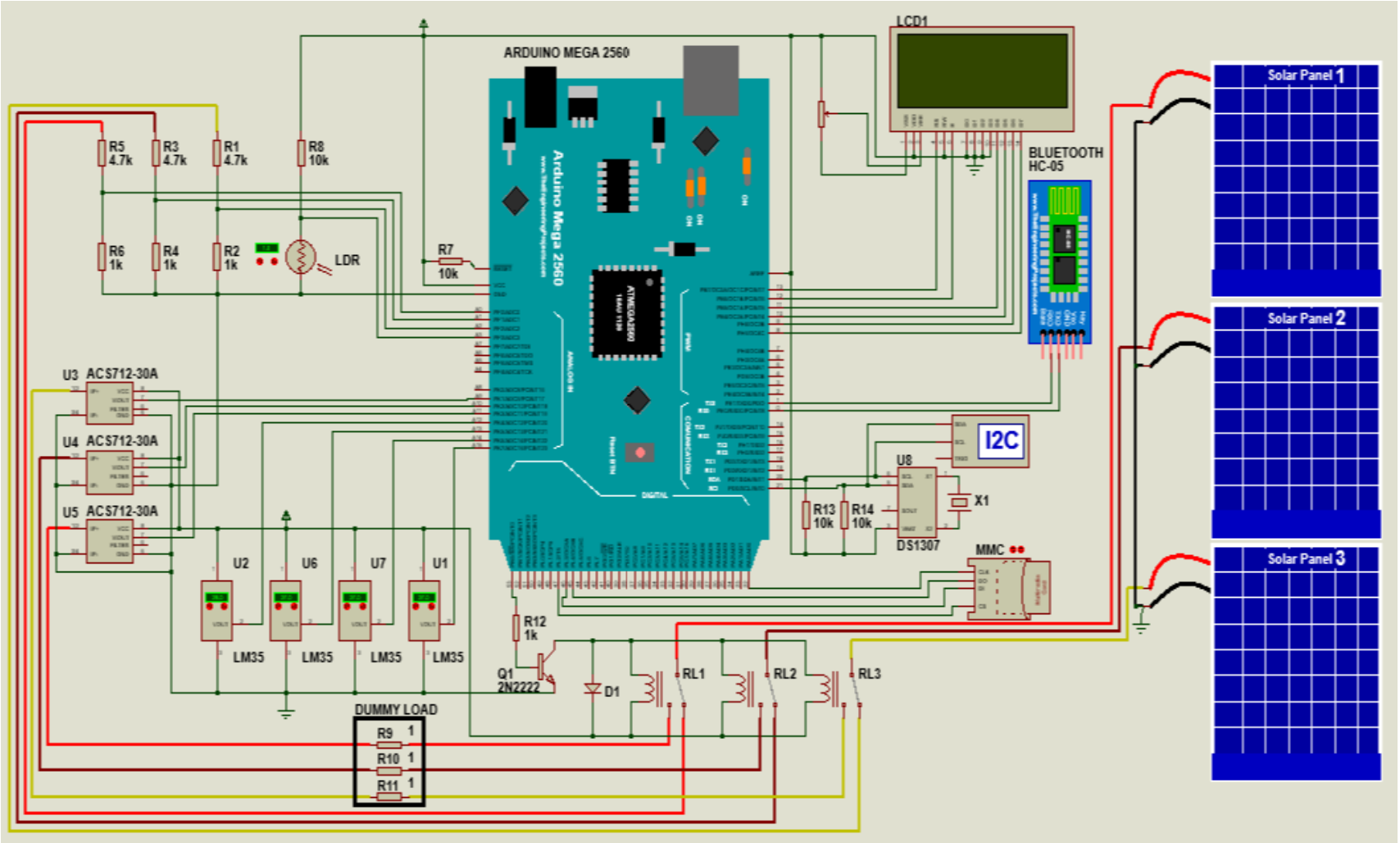

Figure 4: Clad board layout components connections

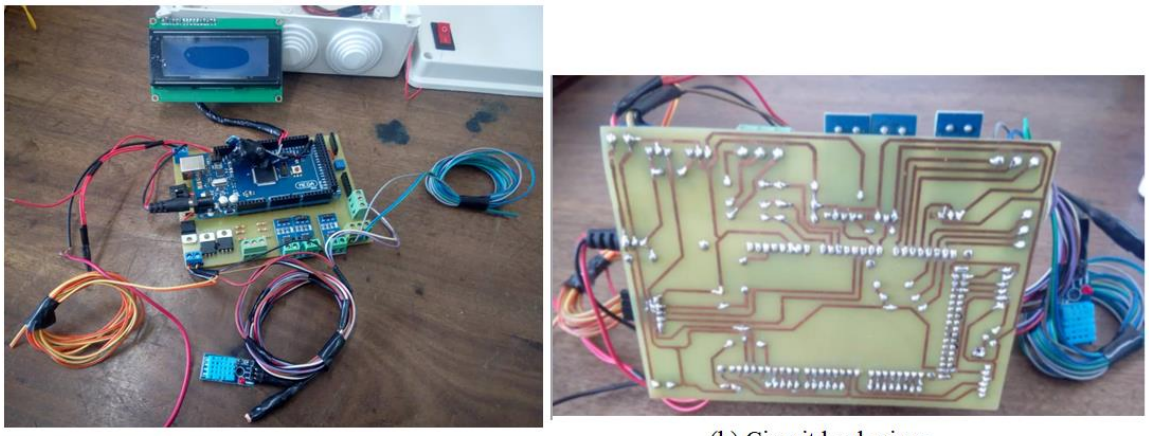

(a) Circuit front view (b) Circuit back view

Figure 5: Clad board circuit with soldered components connections

3.4 Experimental setup

The experimental setup were composed of three polycrystalline silicon SPVP from three different manufacturers and were mounted on the same structure with same equipment and accessories setups as depicted in Fig. 6. The setups shown in Fig. 6 were achieved by developing separate structures (Appendices 2-4) which then were combined to form one structure for experiment (Appendix 5). Experimental work was done on a pitched CMS temporary platform (Fig. 6 / Appendix 5) with varying the gap between the roof and the PVs. It was set on ground at NM-AIST main campus 03.40° south and 036.79° east at the altitude of 1206 meters from sea level facing north the equator. Initial data for an experiment setup were collected from manufacturers' specification; electrical, thermal, and mechanical characteristics as listed in Tables 2, 3 and 4 respectively.

The poles of panel holder (Appendix 2) fixed at 15° panel's inclination adopted from Yadav and Chandel (2013) and Jacobson and Jadhav (2018); were made to slide upwards and downwards in the poles of bottom panel stand (Appendix 3). As a rule of thumb, the selected tilt angle against the horizontal (15°) was appropriate for Arusha-Tanzania where the experiments were conducted. Five holes displaced at 100 mm each with 10 mm diameter were drilled on each bottom panel stand starting at 155 mm from the bottom for interlocking during gap variation. Again, a protractor was used to set the CMS roof holder (Appendix 4) to achieve 20° and 30° slope; hanged using bushes attached to the four poles of a bottom panel stand with the four sides of the sheet holder. Eight millimetre diameter and ten millimetre long pins were used for interconnection between two bushes (from the bottom panel stand and that from sheet holder). The ground levelling was made by the use

of spirit level where as SPVP mounting structure orientation was done using of a Konustar compass.

(a) Front view (b) Rear view

Figure 6: Experimental setup

Table 2: Electrical characteristics of the three solar panels at STC

Electrical characteristics	**Manufacturer**		
	A	**B**	**C**
Cell material	Polycrystalline silicon		
Maximum power (W)	100	100	100
DC open circuit voltage (V)	21.6	21.5	22.14
DC maximum power point voltage (V)	18.0	17.7	18.5
DC short circuit current (A)	6.3	6.2	5.78
DC maximum power point current (A)	5.6	5.7	5.43

Table 3: Thermal characteristics of the three solar panels at STC

Thermal characteristics	**Manufacturer**		
	A	**B**	**C**
Nominal operating cell temperature (NOCT), °C	46 ±2	47 ±2	47 ±2
Temperature coefficient of P_{max} (%)	-0.42	-0.43	-0.45
Temperature coefficient of V_{OC}	-0.32	-0.32	-0.35
Temperature coefficient of I_{SC}	0.05	0.04	0.04

Table 4: Mechanical design characteristics of the three solar panels

Mechanical characteristics	**Manufacturer**		
	A	**B**	**C**
Module dimension (mm)	985 ×701 ×35	1100 × 670 × 35	1100 × 678 ×35
Number of cells	36	36	36
Module weight (kg)	11.0	9	8.8

The DAS was mounted by hanging it under the roof. The DHT-22 and SSN-22e sensors were hanged at the mounting structure for measuring ambient temperature ($\boldsymbol{T_a}$) and relative humidity (***Rh***). Three LM35 temperature sensors labelled $\boldsymbol{T_A}$, $\boldsymbol{T_B}$, and $\boldsymbol{T_C}$ were attached at the back of each panel for measuring rear surface panel temperature of panels A, B, and C. One LM35 sensor labelled $\boldsymbol{T_g}$ was hanged between fore surface of the CMS roof and panel for recording PV-CMS roof gap temperature. One temperature sensor ($\boldsymbol{T_S}$) was placed on the roof fore surface to measure the temperature of CMS front surface. Moreover temperature distribution over the panel B rear surface was measured by three temperature sensors named $\boldsymbol{T_t}$, $\boldsymbol{T_c}$, and $\boldsymbol{T_b}$. The TES 132 USB solar power meter and volt-craft (PL-110SM) were used for solar irradiance measurement and set at same inclination as the solar PV panels to receive simultaneously the same amount of solar energy. Kestrel was fixed perpendicular to the mounting structure for wind speed measurement (Fig. 4). The short currents ($\boldsymbol{I_A}$, $\boldsymbol{I_B}$, $\boldsymbol{I_C}$) and open circuit voltages ($\boldsymbol{V_A}$, $\boldsymbol{V_B}$, $\boldsymbol{V_C}$) were recorded by DAS with help of current and voltage sensors respectively which were integrated into Arduino hardware.

The experiments started at a pitch of 20° for CMS with PV initially laid directly to the roof. The gap variations were done manually. The distance apart was kept increasing by ten centimetres each interval from initial experiment (Fig. 8). This was achieved by sliding the panel holder (Appendix 2) assembly upwards from the roof with an interval of ten centimetres each experiment by interlocking all four poles of panel holder and bottom stand frame as shown in Fig. 6. Roof pitch was changed manually by interlocking front side of roof holder and the two bottom panel stand poles (Fig. 6a) at already set positions.

Each solar PV panels was cleaned with clean water using a soft cloth every day before starting the experiment. The experiments were conducted from 27th to 30th August 2018, 06th to 11th September 2018, 14th to 21st September 2018, 01st, 11th to 24th, 27th of October 2018, and 11th, 13th, 18th of November 2018 commencing at hours with clear sky.

3.5 Experimental measurements

3.5.1 Irradiance variation during the test days

To consider the impact of irradiance variation; TES 132 USB solar power meter and volt-craft (PL-110SM) were set at same inclination as SPVs to receive same amount of irradiance as captured by the module. Solar irradiance readout form both device were taken and compared for reliability of the data obtained. Under this section, parameters such as irradiance $\boldsymbol{G}$, ambient temperature $\boldsymbol{T_a}$, and relative humidity $\boldsymbol{Rh}$ were monitored. The $\boldsymbol{Rh}$ and Ta readouts were done by and served in SSN-22e temperature- humidity data logger. Irradiance for some days was plotted for comparison whilst outdoor solar panels performance at different irradiance was investigated. Measurements were taken during dry season hence the effect of precipitation was not taken into consideration.

3.5.2 Impact of CMS on PV panel performance

To consider the impact of CMS roof temperature on the PV panel performance, one panel was laid directly on the roof. Temperature distribution over the panel area was monitored using two sets of temperature sensors (three LM35 sensors and three USB temperature data logger-SSN 11e). Parameters such as panel B temperature $\boldsymbol{T_B}$, PVs CMS gap $\boldsymbol{T_g}$, CMS temperature $\boldsymbol{T_S}$, panels' distribution temperatures $\boldsymbol{T_t}$, $\boldsymbol{T_c}$, and $\boldsymbol{T_b}$, and irradiance $\boldsymbol{G}$ were monitored and continuously recorded by the PC via Bluetooth using a Tera Term software at time interval of about 2 minutes.

Again, three panels were fixed on the frame stand (Fig. 7) for investigating the panel-CMS roof gap influence from every panel. Three closely identical strings of load resistance were made purposely for PVs' electrical characteristics consideration and were connected to a individual panel, ammeter (A), and voltmeter (V) as shown in Fig. 8. Panel stand (with panels mounted) was then left at zero centimetre gap as depicted in Fig. 7, the performance was made at irradiance of 480±10, 680±10, and 820±10 Wm-2 of the same day. The operating parameters such as open circuit voltages, short circuit currents, ambient temperature $\boldsymbol{T_a}$, PV- CMS gap $\boldsymbol{T_g}$, panels' temperatures $\boldsymbol{T_A}$, $\boldsymbol{T_B}$, and $\boldsymbol{T_C}$, and irradiance $\boldsymbol{G}$ were monitored and continuously recorded by the PC via Bluetooth using a Tera Term software at time interval of about 2 minutes. Short circuit currents and open circuit voltages for electrical characteristics were measured by digital multimeter manually (Fig. 9) captured using digital camera.

Figure 7: Solar PVs mounted on panel holder at 0 cm from CMS

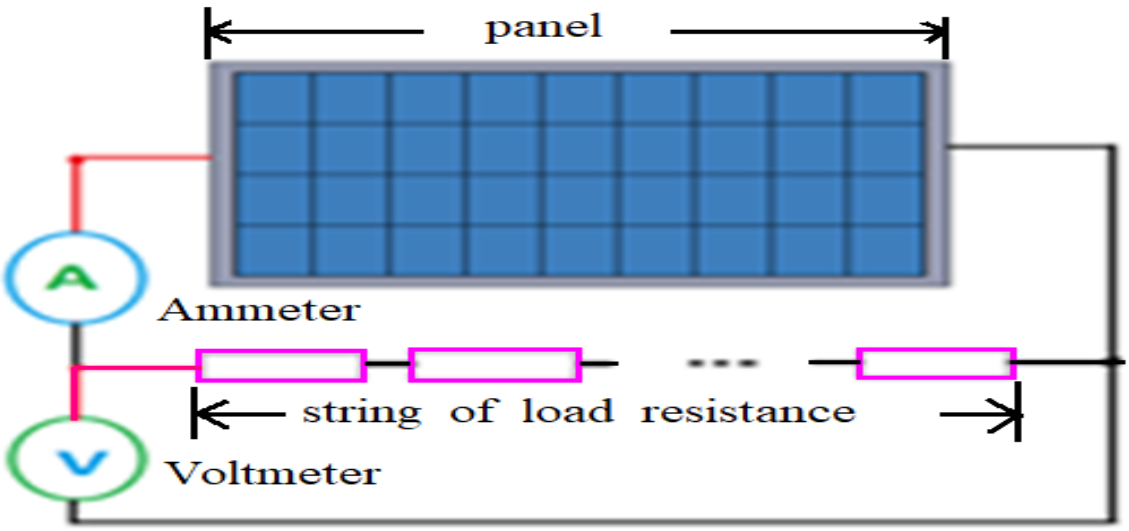

Figure 8: Circuit diagram for I-V curves measurements

Figure 9: I-V experimental data collection

3.5.3 Effect of variance in gap on PV performance

Panel stand (with panels mounted) was then raised up at the intervals of ten centimetres from zero to fifty centimetres as shown in Fig. 6. Once again, the three strings of load resistance (Fig. 8) for each solar PV were used to perform PVs' electrical characteristics. The operating parameters such as open circuit voltages, short circuit currents, ambient temperature $\boldsymbol{T_a}$, PV CMS gap $\boldsymbol{T_g}$, panels' temperatures, and irradiance $\boldsymbol{G}$ were monitored and continuously recorded by the PC via Bluetooth using a Tera Term software at time interval of about 2 minutes. Short circuit currents and open circuit voltages for electrical

characteristics were measured by digital multimeter manually (Fig. 9). The performance was made at irradiance of 820±10 Wm^{-2} of the same day same hour.

3.5.4 SPVP Matlab simulation

The SPVP output voltage is a function of the photocurrent that mainly determined by load current depending on the incident solar radiation level during the operation. I-V characteristics curve are nonlinear which they vary with PV cell temperature and solar irradiation. The fundamental parameters related to solar PV panel characteristics are short circuit current and open circuit voltage. From Fig. 3 which is the generalized model for equivalent circuit, consisting of a current source (I_{PV}) connected in anti parallel with a diode (D), a shunt resistance (R_P) expressing a leakage current (I_P) and a series resistor (R_S) describing an internal resistance to the current flow. The output of the current source is directly proportional to the light falling on the solar PV cell. The solar cell produces neither a current nor voltage during darkness. Basing on Fig. 3, the photo current of solar PV cell can be calculated as

$$Ipv = Id + Ip + Io \tag{3.1}$$

where I_{PV} is a light-generated current, I_d is diode saturation current, I_p is a shunt current and I_o is the output (load) current.

A double exponential mathematical description model is not taken into account due to some restrictions; the single diode model was based on the assumption that the recombination loss in the depletion region is absent. The light produced current of a PV cell depends on an incident solar radiation level and its working temperature which can be expressed by expression (3.2).

$$Ipv = [Isc + K\text{cc}(T\text{-}T_o)]G \tag{3.2}$$

Which can further be simplified

$$Ipv = Iph\ (To) + Kcc\ \ (T - To) \tag{3.3}$$

$$Iph\ (To) = Isc\ (To)\frac{G}{Go} \tag{3.4}$$

$$Kcc = [Isc\ (Tw) - Isc\ (To)]/(Tw - To) \tag{3.5}$$

where I_{ph} is a photo current, *Isc* is the PV cells' short circuit current at STC, *Kcc* is the cells' short circuit current temperature coefficient, *T* and *Tw* are the PV cells' absolute temperature, *To* is the cells' reference temperature at STC, and *G* is the solar irradiance in Wm^{-2} (Tsai *et al*., 2008; Mohammed, 2011; Bellia *et al*., 2014).

Again, the diode saturation current varies with cell temperature as described in equation (3.6)

$$Id = Isr\left(\frac{T}{To}\right)^{3/n} \exp[\frac{qEg\left(\frac{1}{To}-\frac{1}{T}\right)}{nk}] \quad (3.6)$$

Expression (3.6) can be again rewritten as

$$Id = Id(To) \times \left(\frac{T}{To}\right)^{\frac{3}{n}} e^{\frac{qEgTo}{nk\left(\frac{1}{T}-\frac{1}{To}\right)}} \quad (3.7)$$

$$Id\ (To) = Isc\ (To)/e^{\frac{qVoc\,(To)}{nkTo}} - 1 \quad (3.8)$$

where *Isr* = I_d*(To)* is the reverse saturation current of the cell at STC, *Eg* is the semiconductor's cell band energy gap, *n* is an ideal factor-dependent on technology (*n* = 1.3 for silicon polycrystalline), *k* is a Boltzmann's constant (*k* = 1.38 x 10^{-23} J/°K), *q* is an electron charge (*q* = 1.602 x 10^{-19} C) (Park *et al*., 2014; Muzathik, 2014; Bonkoungou, 2015).

Diode saturation current (I_d) and photo current (I_{pv}) are temperature dependant, increasing accuracy in expression (3.1) temperature is to be taken into consideration. The shunt resistance (R_P) is contrariwise correlated with shunt current to the ground. Generally, the SPVM productivity is insensitive to variation in R_P and the shunt resistance can be assumed to approach eternity without leakage current to ground. Any small deviations in R_S will significantly disturb the PV output power. Therefore, Equation 3.1 can be rewritten as equation 6 of Bellia *et al*. (2014). Neglecting leakage current through shunt resistance, and make a use of equations 3.2 through 3.8 above, the output current (I_O) of the solar PV cell becomes

$$Io = Isc\,(To)\frac{G}{Go} + \frac{Isc\,(Tw) - Isc\,(To)}{Tw - To}[T - To] - \left[\frac{Isc\,(To)}{e^{\frac{qVoc\,(To)}{nkTo}} - 1} \times \left(\frac{T}{To}\right)^{\frac{3}{n}} e^{\frac{qEgTo}{nk\left(\frac{1}{T} - \frac{1}{To}\right)}}\right][e^{\frac{q(Vo + IoRs)}{nkT}} - 1] \quad (3.9)$$

where Vo is an output voltage, and R_S is a series resistance.

Equation (3.9) is known as a single exponential derived from the physics of the PN junction which models a solar PV cell and is reflecting the characteristic of the cell. The included series resistance (R_S) represents the internal resistance of each in the connection among cells

$$Rs = -\frac{dV}{dIvoc} - \frac{1}{Xv} \quad (3.10)$$

$$Xv = Id\,(To) \times \frac{q}{nkTo} \times [e^{\frac{qVoc\,(To)}{nkTo}} - 1] \quad (3.11)$$

The output voltage of the SPVP is a function of the light generated current that mostly determined by output current depending on the incident solar radiation level during working.

$$Vo = \frac{nkT}{q} ln \frac{Ipv}{Id} \quad (3.12)$$

The parameters are as defined in equations 3.1 through 3.9 (Tsai *et al*., 2008; Mohammed, 2011; Bellia *et al*., 2014; Park *et al*., 2014; Muzathik, 2014; Bonkoungou, 2015).

The Matlab function written hereunder (Appendix 6 and Appendix 7) is providing the I-V curves at different panel's temperature and altered irradiance. The constant inputs were defined, and later the expression 3.2, 3.3, 3.4, 3.5, 3.8, 3.10, and 3.11 were written. Experimental data and some manufacturer specifications in Table 3.2 were used as input for mathematical model. Experimental and theoretical I-V curves were compared.

3.5.5 Effect of partial shading on SPVPs

To examine shading; partial shading were applied under varied illumination conditions. Different hardware outdoor setup tests were conducted for each panel with similar and dissimilar shading shape pattern materials. Shading the panels with similar type of material

is regarded as common shading in this study whilst applying dissimilar material for each panel shade is regarded as uncommon shading. The main differences among the common and uncommon shading materials were in their ability to block solar irradiance to reach the PV cells. Common shading were done following ~3 to 100 % for panels A and C while shading for panel B started when panels A and C reached 89 % of shade. Panel B was left un-shaded from ~3 to 78 % of shading in order to compare electrical output parameters. Uncommon shading was done from ~3 to ~16 % for all panels. Above 16 % of shade, only panel A and B were considered. No current was generated by panel C when shading exceeded 16 %. White paper was used for common shading whilst foliage, white paper, and opaque object were used for panel A, B, and C respectively for uncommon shade. The selected materials are most likely to cause shade either due surrounding objects or gale which lifts various materials when blows.

Common shadings started by covering a single cell from the bottom of the panels and keeping increasing the number of cells upwards. For uncommon, it started by covering one cell whilst the second activity was 6 % which was attained by considering two cells. Third activity was achieved by considering the six cells whereas last test shading was for twenty cells. The parameters such as open circuit voltages, short circuit currents and irradiance readout were taken.

CHAPTER FOUR

RESULTS AND DISCUSSION

4.1 Introduction

This chapter presents data obtained from experimental and theoretical analysis. They are presented in relation to the specific objectives of the study. Sections 4.2 - 4.4 are about the first objective, to evaluate the performance of standalone SPVP on natural air passive cooling by varying gap between pitch CMS roof and panel. It includes the variation of irradiance on test days, the impact of CMS roof on performance of the PVs at different irradiance, the effect of variation in gap on PVs performance. Section 4.5 is about second objective, that is simulation and the last section 4.6 is about third objective, partial shading.

4.2 Irradiance variation during the test days

To consider the impact of irradiance variation, solar irradiance readouts from two devices, TES 132 USB solar power meters and volt-craft (PL-110SM), were taken and compared for reliability of the data obtained (Fig. 10). One can see the data agree well generally between each other; still the variance in the range of 13 to 23 Wm^{-2} is observed at low irradiance (below ~500 Wm^{-2}), and discrepancies are rising up to 96 Wm^{-2} at higher solar energy. Since the TES 132 meter provided more stable signal as well was able to store data its readouts were taken to analyse the impact of irradiance variation and displayed in the next sections. Irradiance readouts were captured and stored direct to PC every second.

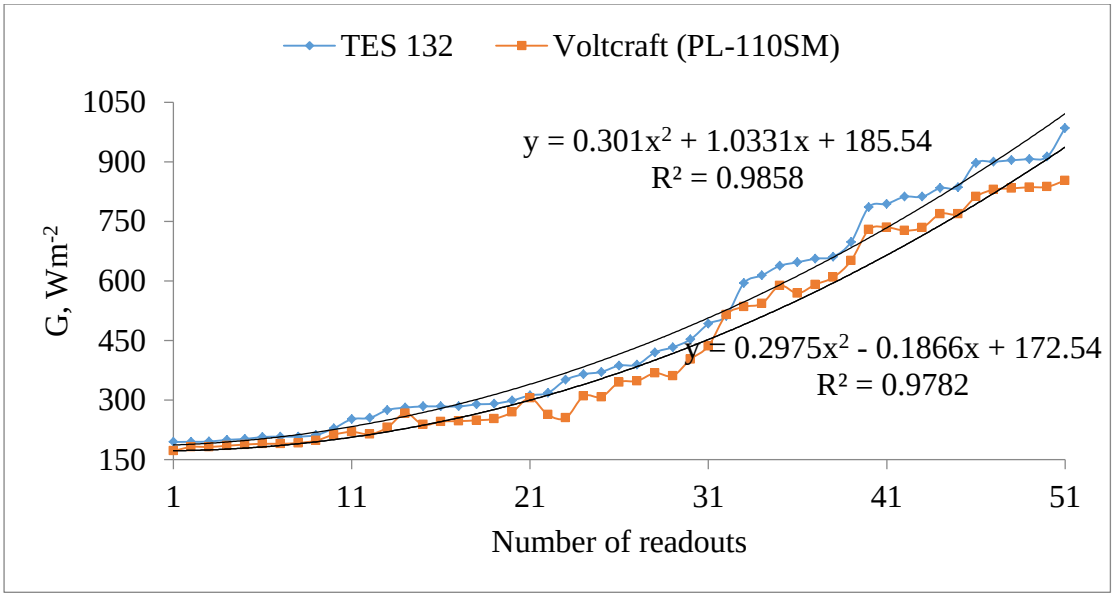

Figure 10: Comparison of readings from two solar meters, TES 132 USB and volt-craft PL-110SM

During testing, data recorded and considered for analysis were those taken at clear sky condition when less insolation variations was expected as compared to cloudy hours. The clear sky provided high and steady irradiance nearly to STC. Bouncing variations in irradiance can be seen almost instantaneously as recorded for several days as depicted in Fig. 11. Scattered cloud conditions for some of the hours of a days caused fluctuations in irradiance. It was challenging to carry tests due to the variation of irradiance reaching the surfaces of the solar PV panels; the observation which concur with Sirisamphanwong and Ketjoy (2012) study. The irradiance was reduced sharply when sun was covered by clouds and raised abruptly when cleared. The variations created adamant situations due to complexity in coping up with sudden cloud movement. However, readouts resulted from persisted cloud cover were not taken into consideration.

Weather parameters; ambient temperature $\boldsymbol{T_a}$ and relative humidity ***Rh***, were recorded. Figure 12 shows the variations of $\boldsymbol{T_a}$ and ***Rh*** versus measured solar irradiance in ascend sorted. Either air temperature or humidity exhibited slight influence by solar power; temperature increases and humidity decreases with irradiance rise but not considerably. The readouts of $\boldsymbol{T_a}$ ranged from 23 °C – 35 °C, and of ***Rh*** about 31% to 80% throughout test days. At the same time antiphase variations between the $\boldsymbol{T_a}$ and ***Rh*** were distinctly observed. It was noted that any drop in panels' temperatures whilst irradiance keeping increasing were due to an upswing in ***Rh***. Furthermore, increased wind blowing from 0 to 2.4 ms^{-1}

contributed to diminution in temperature. Any drop in solar irradiance there was a noticeable reduction in panels' current and voltage, at the same time the panels' temperature and ambient temperature also dropped similar results were reported by Arjyadhara *et al*. (2013). A high decline in ***Rh*** was a result of increased T_A, T_B, T_C, and T_a and vice versa.

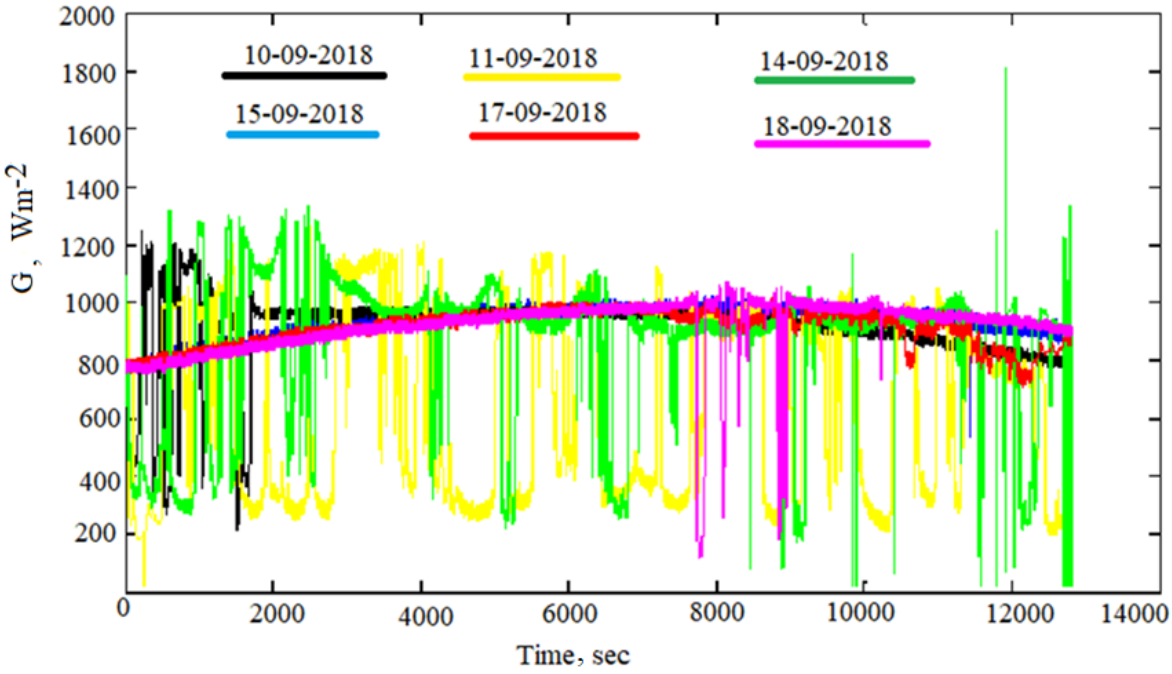

Figure 11: Irradiance at different test days

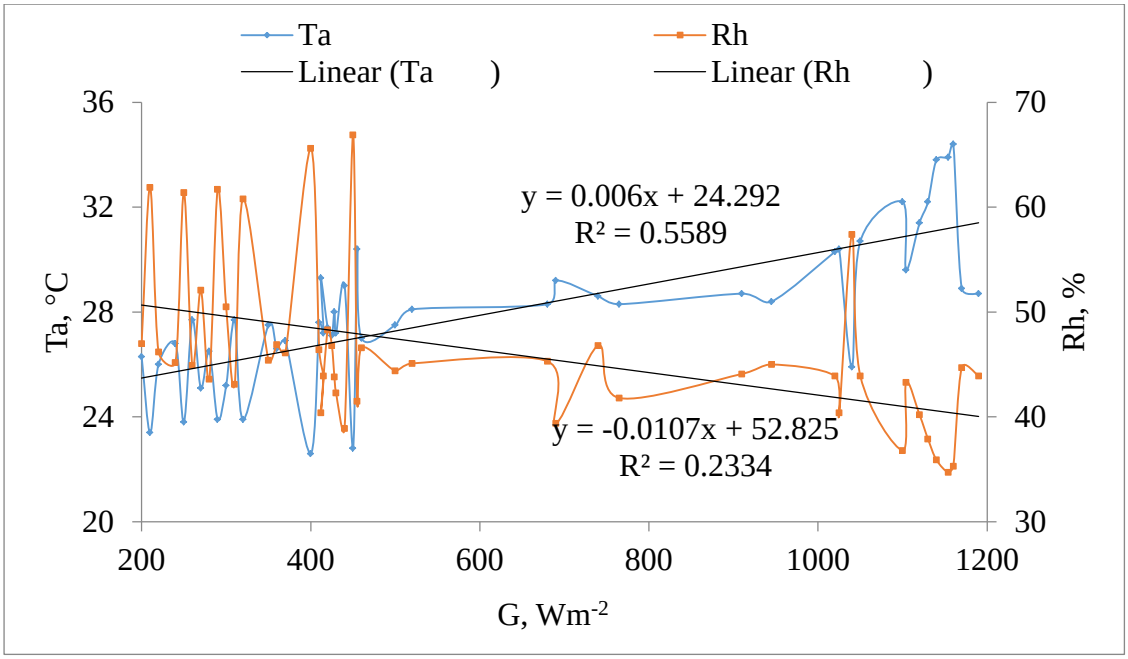

Figure 12: Variation of Ta and Rh versus irradiance

4.3 Impact of solar irradiance and CMS roof on PV panel performance

Solar radiation, ambient temperature, mounting structure, panel material composition, and wind speed are factors said to affect the PV operating temperature (Armstrong and Hurley, 2010). The impact of CMS roof on PVs' temperature was monitored only on panel B which was laid on CMS roof directly. Other two panels were removed so as to avoid roof shading and imitate typical maintenance of a solar panel on the roof. As mentioned in section 3.5.2; temperature distribution over the panel area was monitored using two sets of temperature sensors (three LM35 sensors and three USB temperature data logger-SSN 11e). The observed temperature values differences from the two sets of sensors were within ± 3% which is insignificant difference and ensures reliability of the data obtained. Temperature measured were $\boldsymbol{T_a}$, $\boldsymbol{T_S}$, $\boldsymbol{T_g}$ and $\boldsymbol{T_B}$. Moreover, temperature distribution ($\boldsymbol{T_b}$, $\boldsymbol{T_c}$, and $\boldsymbol{T_t}$) on rear surface of panel B as indicated in Fig. 6b (the centered panel) was evaluated.

Under different weather conditions it was noted that CMS were temperature absorbing material where $\boldsymbol{T_S}$ reached 62 °C, $\boldsymbol{T_g}$ was 48 °C and $\boldsymbol{T_B}$ was 74.5 °C which were the highest temperatures under this study whilst $\boldsymbol{T_a}$ was ranging from 30-34 °C. The CMS temperature can be radiated quickly and make a rise in PV panel temperature if not cooled. The rise in temperature of the solar PV panel was contributed by the absence of no air exchange on the rear side coinciding with the findings reported by Dominguez *et al*. (2011). For every abrupt upsurge in $\boldsymbol{T_B}$ also there were a sharp rises in $\boldsymbol{T_S}$ but only small rise in $\boldsymbol{T_g}$. It was noted less $\boldsymbol{T_S}$, $\boldsymbol{T_g}$, and $\mathbf{T_B}$ before 10:30 hours and after 15:00 hours compared to noon hours which were ranging between 60 to 74.5 °C for $\boldsymbol{T_B}$ as seen in Fig. 13, the figures which were also reported in Kaldellis *et al*. (2014). It is obvious that $\boldsymbol{T_B}$ increased due to negligible gap as a result $\boldsymbol{T_g}$ was increased. Destructive effects to the panel may occur if high $\boldsymbol{T_g}$ persists. Fluctuations for monitored parameters were due change in environmental conditions caused by either among the following; increased or decreased wind speed, un-prolonged cloud cover, or irradiance fluctuations which was ranging from 300 to 1150 Wm^{-2}.

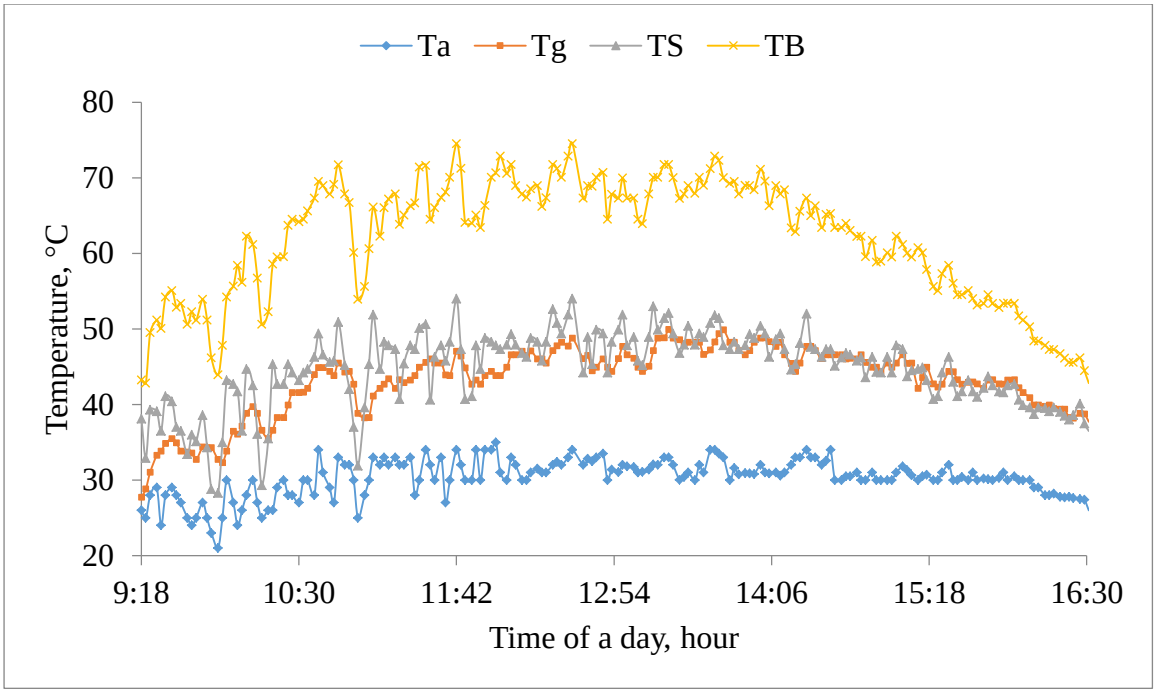

Figure 13: Variations of temperatures versus time of a day

Any variation in irradiance was affecting the panel's temperature distribution and $\boldsymbol{T_S}$. The highest encountered $\boldsymbol{T_b}$ was 72 °C which is much close to that reported by Kaldellis *et al*. (2014). During the exercise, none of the three parts of the panel found to have equal temperature (Fig. 14); the differences were ranging from 0.083 to 8.89 % referencing to $\boldsymbol{T_c}$ with highest difference of 5.86 °C which is closely related to study reported by Lee and Tay (2012). Almost 62 °C was the highest temperature CMS roof recorded. The negligible gap among the PV and CMS roof exaggerated the raise in $\boldsymbol{T_g}$ to 48 °C (space between the PV back sheet to the PV frame edge was considered in this case). Heat removal underneath the panel was unsupportive due to insignificant gap, the finding which concurs with Dominguez *et al*. (2011). Upsurge in irradiance and reduced *Rh* were the origin for an escalating of the measured parameters. Solar PV panel temperature did not decline at high irradiance with small wind speed the results which were also observed by Koehl *et al*. (2011). The high solar PV panel temperature measured led to 6.78 A which was almost 9.35% excessive DC short circuit current from laboratory work.

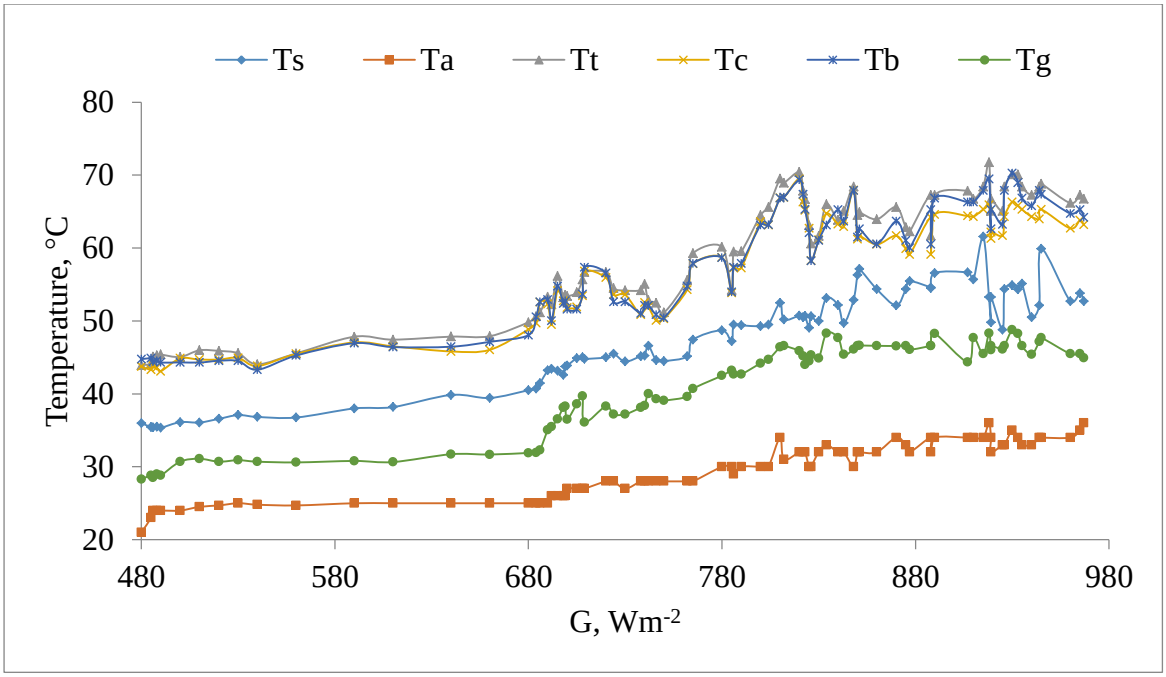

Figure 14: Temperature distribution over the system with the panel B mounted directly on the roof

Impact of solar irradiance on three solar PV panels performance is considered in this section. It is well known that temperature is one of crucial factors which also influence solar cell performance; therefore the three panels' temperatures were also monitored thoroughly. Plots for the panels' temperatures $\boldsymbol{T_A}$, $\boldsymbol{T_B}$, $\boldsymbol{T_C}$ versus irradiance are shown in Fig. 15. Similarly as in Fig. 14 definite ascending trend with irregular oscillations is seen in the plots. Nevertheless behavior of the three quantities is rather synchronic. As it is mentioned above fluctuations in the panels' temperatures can be attributed to humidity and wind speed variations. Worth to notice also some difference in temperatures between the three panels; $\boldsymbol{T_A} > \boldsymbol{T_C} > \boldsymbol{T_B}$; that difference keeps disregarding irradiance. At the same time the ambient temperature was about 32 °C (Fig. 14) at irradiance 820 ±10 Wm^{-2}; the solar panel temperature exceeds the ambient one by 28 °C – 35 °C that is much higher than usually accepted about 15 °C. This higher temperature of the solar PV panels can be attributed to closely spaced roof surface which apparently brings extra heating the panels. Similar observation was reported in Kaldellis *et al*. (2014); that panels operates at different range of temperature whereas 70 °C was encountered and this remained due to poor cooling. Increased wind speed at higher irradiance caused the panels temperature to be almost constant instead some small variations.

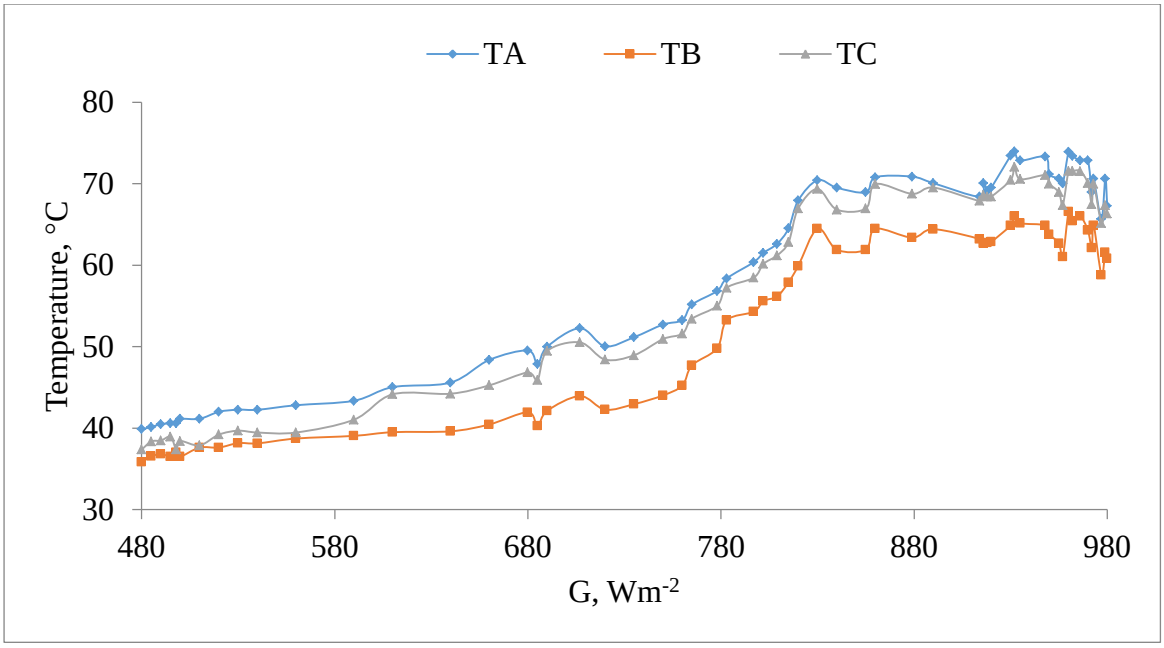

Figure 15: Panels' temperature variation versus irradiance

Impact of solar irradiance on electrical performance of the solar PV panels was investigated. The outdoor measurements of current and voltage were done on the panels fixed directly on roof as shown in Fig. 7. Electrical parameters; short circuit currents $\boldsymbol{I_A}$, $\boldsymbol{I_B}$, $\boldsymbol{I_C}$ and open circuit voltages $\boldsymbol{V_A}$, $\boldsymbol{V_B}$, $\boldsymbol{V_C}$ were plotted against irradiance in Fig. 16 and Fig. 17. The currents grow linearly with irradiance increase whilst voltages drop by 0.7-1.0 V at irradiance approaching 820 ±10 Wm^{-2}. These results are in accord to linear relation of current to illumination

$$I(G) = \left(\frac{G}{Go}\right)[Io(Go)] \qquad (4.1)$$

Where Go is 1 kWm^{-2} at AM 1.5, I_0 (Go) cell current at Go; and logarithmic dependence of voltage (Mekhilef *et al*., 2012).

Figure 18 shows a complete I-V curves measured for the three panels and displayed at three different irradiance 480±10 Wm^{-2}, 680±10 Wm^{-2}, and 820±10 Wm^{-2}. The nonlinear behavior of SPVP cell is apparent, that the output current and power of SPVP cell be influenced by the cell's terminal operating voltage and temperature, and solar irradiance as well. The values of maximum power obtained from the curves were plotted against irradiance in Fig. 19. It was clear from Fig. 16, 18, and 19 that when solar irradiance increases, the short circuit currents and maximum powers were keeping increasing due to increased number of photons reaching the modules. The reason is the open circuit voltage is logarithmically reliant on the solar irradiance; nevertheless the short circuit current is

directly proportional to the radiant intensity. If we compare the three panels performance, one can notice the interrelation between the parameters; $\boldsymbol{I_A} < \boldsymbol{I_B} < \boldsymbol{I_C}$, $\boldsymbol{P_A} < \boldsymbol{P_B} < \boldsymbol{P_C}$, $\boldsymbol{V_A} > \boldsymbol{V_B} > \boldsymbol{V_C}$; hence the output power is mostly influenced by current change and least by voltage. Furthermore, a link of electrical parameters to panels' temperature should be admitted here; highest $\boldsymbol{T_A}$ – lowest $\boldsymbol{I_A}$ – lowest $\boldsymbol{P_A}$ – (in-spite of highest $\boldsymbol{V_A}$ Fig. 17), nevertheless lowest $\boldsymbol{T_B}$ doesn't correspond to highest $\boldsymbol{I_B}$ and $\boldsymbol{P_B}$; but intermediate.

It's apparently short circuit current, open circuit voltage and net power varied with solar PV panel temperature for constant irradiance. The results accord with Tsai *et al*. (2008), Tyagi *et al*. (2013), Bellia (2014), Bonkoungou (2015) and Fara and Craciunescu (2017) theoretical work studies that with rise in working panel temperature, short circuit current increases whilst the open circuit voltage and net power decreases. Generally it was thought-provoking to conduct electrical characteristic tests due to variation of irradiance reaching the surfaces of the PVs that varies from morning to afternoon as also observed by Sirisamphanwong and Ketjoy (2012). A big range of irradiance without change in readout are seen from Fig. 16 and Fig. 17, this was due to rapid rise in irradiance. In every drop in solar irradiance there was a reduction in $\boldsymbol{I_A}$, $\boldsymbol{I_B}$, $\boldsymbol{I_C}$, $\boldsymbol{V_A}$, $\boldsymbol{V_B}$, and $\boldsymbol{V_C}$, at the same time the $\boldsymbol{T_A}$, $\boldsymbol{T_B}$, $\boldsymbol{T_C}$, and $\boldsymbol{T_a}$ also dropped. Related observations were reported by Arjyadhara *et al*. (2013) that with the increasing irradiance both the open circuit voltage and short circuit current increases and hence the maximum power varies whereas I-V curves also varies. All curves from the panels were found to have similar trend with increased output parameters when the irradiance was improved. Similar observations were reported by Tsai *et al*. (2008), Bonkoungou *et al*. (2013), Park *et al*. (2014) and Bellia *et al*. (2014) study.

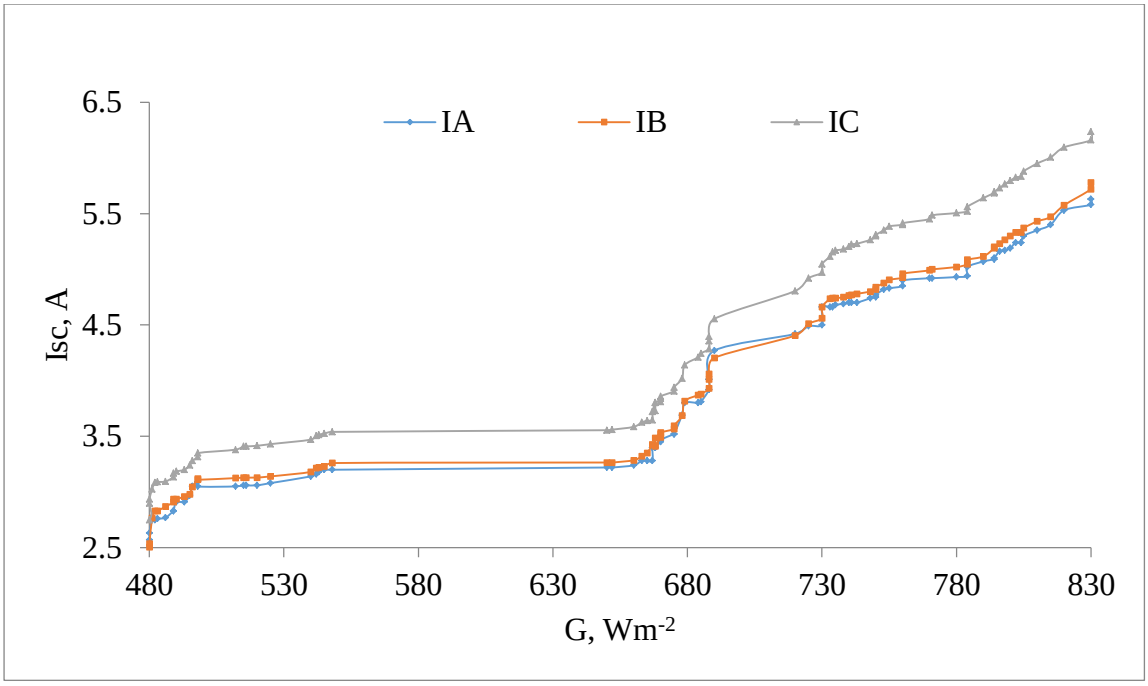

Figure 16: Short circuit currents for three solar panels versus irradiance for h = 0

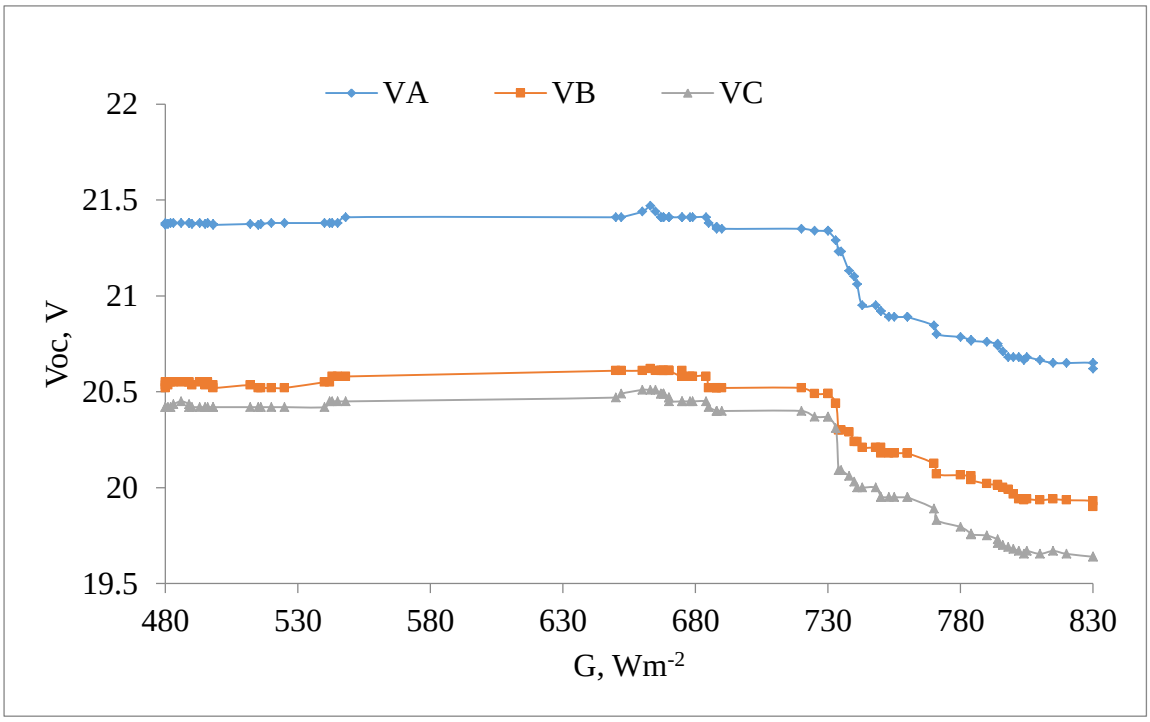

Figure 17: Open circuit voltages for three solar panels versus irradiance for h = 0

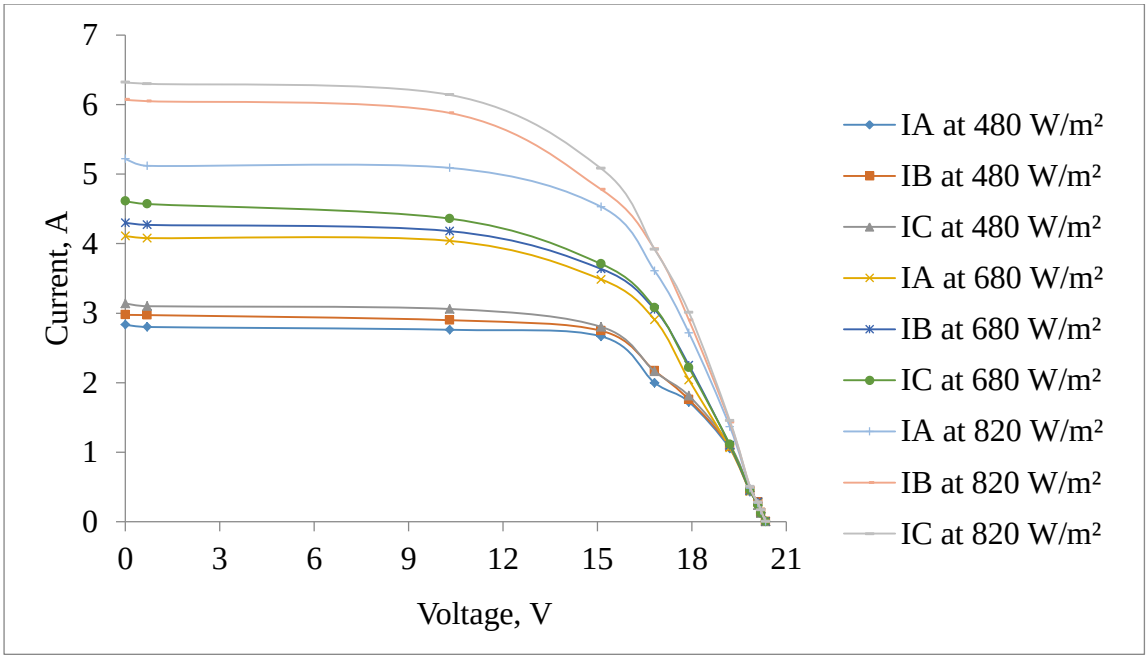

Figure 18: I-V curves for three solar panels at different irradiance for h = 0

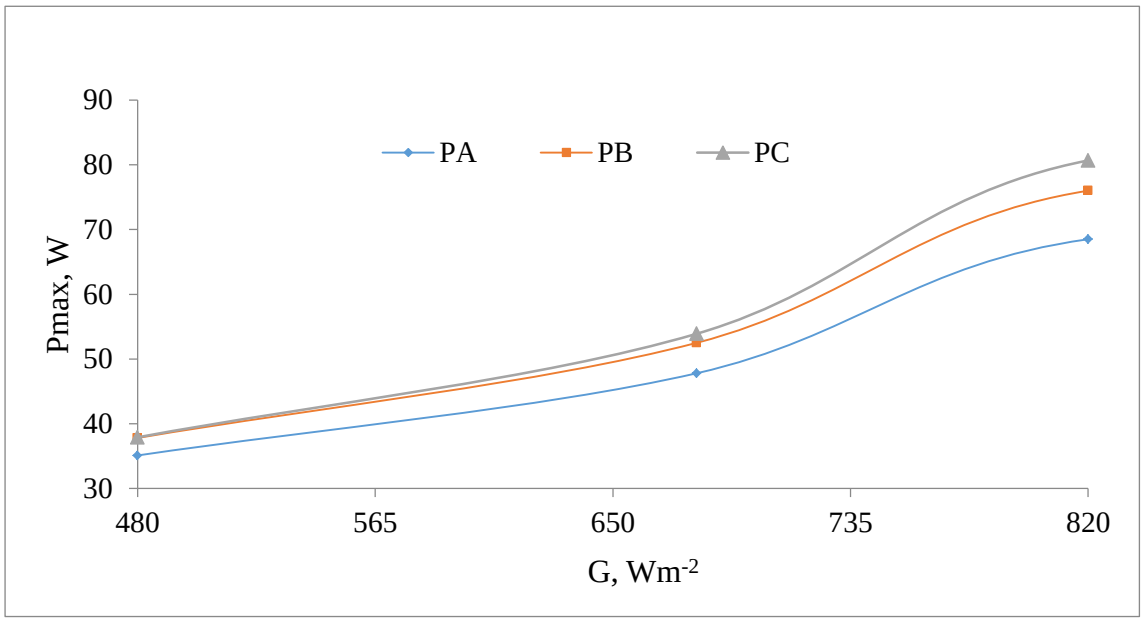

Figure 19: Variation of maximum power versus irradiance for h = 0

4.4 Effect of variance in gap between CMS roof and panel on PV performance

Effect of gap alteration between the CVS roof and panels on the PV panel performance was considered in this section. Temperatures of the rear center panels, in between roof-PV gap ($\boldsymbol{T_g}$), and ambient temperature ($\boldsymbol{T_a}$) were also monitored (Fig. 20). The measurements were

performed at solar irradiance 820±10 Wm^{-2} on the same day same hour and the gap size varied from zero to 50 cm.

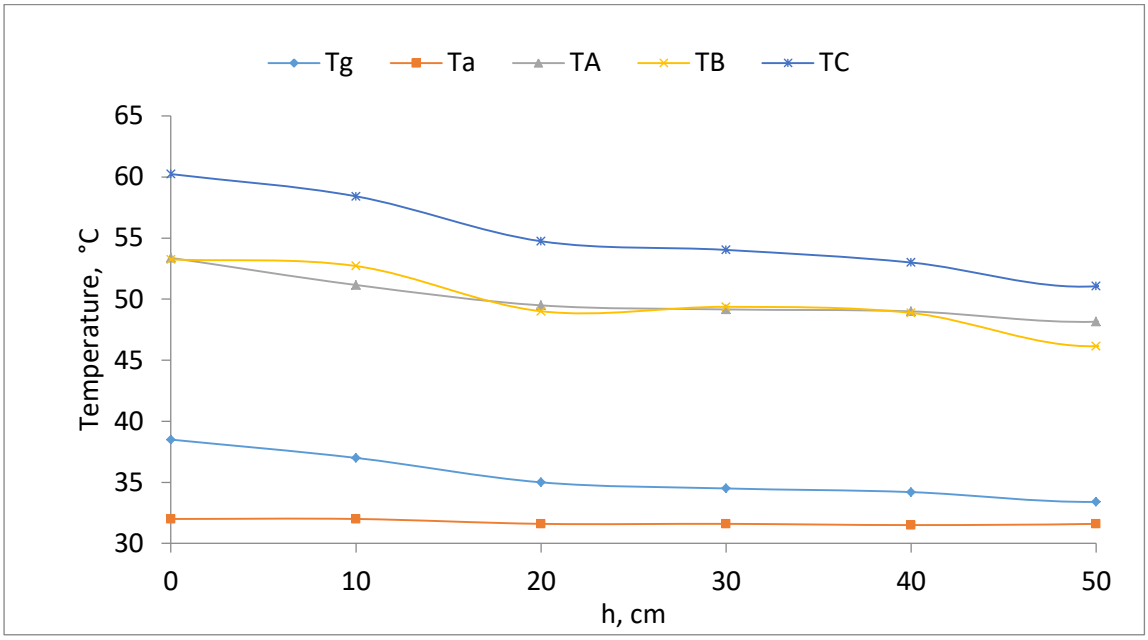

Figure 20: Temperature variation depending on gap alteration from h=0 -50 cm at G=820±10 Wm^{-2}

One can see the panels' and in gap temperature decrease gradually with the gap enlarge from zero to 50 cm while ambient air temperature doesn't change. Photovoltaic-CMS roof gap temperature was lower than the back panel temperature but higher than the ambient temperature; this result concurs with Dominguez *et al*. (2011). Gap temperature was decreasing after every gap rising. None of them succeeded to be similar throughout the measurement though in some cases the dissimilarities were insignificance. It was detected that mounting the panel at 50 cm gap would reduce panels' temperature to ~21% depending on surrounding $\boldsymbol{T_a}$. The PV panel might have less than 45 °C at 50 cm PV- CMS roof gap if the Rh ranges from 31 to 80 % as revealed in other tests of the same study (Section 4.1).

The measured panel temperature can be obtained also theoretically using expression 2.4 (Mekhilef *et al*., 2012; Schwingshackl *et al*., 2013). Computing the cell temperature using expression (2.4) above, panels' temperature were supposed to be in range of 47.6 °C to 50.9 °C for $\boldsymbol{T_A}$ whilst 48.4 °C to 51.7 °C for $\boldsymbol{T_B}$ and $\boldsymbol{T_C}$ depending on irradiance and ambient temperature. At h=50 cm the $\boldsymbol{T_a}$=32 °C and $\boldsymbol{G}$ = 820 Wm^{-2}, for all panels' measured temperatures were in computed range. Also the panel's temperature readouts at 30 ° CMS pitched roof at h=50 cm were in the range of NOCT. The panels' temperature for h=0 was in

range of 54 °C to 60 °C though it could go beyond that if the panels are to be left at h=0 for long time as already depicted in section 4.3. The disagreement in calculated and measured temperatures could be contributed to roofing material's impact as well as less gap. A similar observation on ventilation was reported by Skoplaki and Palyvos (2009) that, higher panels' temperature is due to lack of proper cooling that results from poorly ventilated backside which also depends on the mounting structure for a given solar irradiance.

Electrical performance of the solar PV panels was analised and the results were presented in Fig. 21 to 24. The curves were found to be disparate throughout though all they got similar trends found in literatures. With the gap expand from zero to 50 cm, short circuit current of each panel (Fig. 21) was observed to be higher at 0 cm gap. There were slight current diminutions in the next three gap variation whereas after it started to rise. Maximum power current of each panel slightly ascends with the gap enlarge (Fig. 21). Maximum power was raised by ~5-11% (Fig. 24), maximum power current by ~4-5%, whilst efficiency and fill factor were snowballing per gap rise (Fig. 25 and Fig. 26). When the effect of tolerance and a recommended typical temperature reduction factor are considered, every panel was supposed to generated at least 86.33 W but only panel C approached (Chikate and Sadawarte, 2015). Open circuit voltages were increasing while the gap expanded as panels' temperatures were dropping (Fig. 22). The I-V curves in Fig. 23 were presented for 0 and 50 cm gap to avoid over-crowding. The increase in open circuit was significant to raise power output. Generally; the open circuit voltage, fill factor and maximum power decreased with temperature where as short circuit current increased. It was noticed that the temperature coefficient of the open circuit voltage, fill factor and maximum output power was negative whilst positive for the short circuit current. Comparable observation was reported in Dubey *et al.* (2013), Chander *et al*. (2015), Tyagi *et al*. (2013) and Mattei *et al*. (2006) who revealed that with increased panel temperature; the short circuit currents increased whilst open circuit voltages, output power as well as efficiency declined.

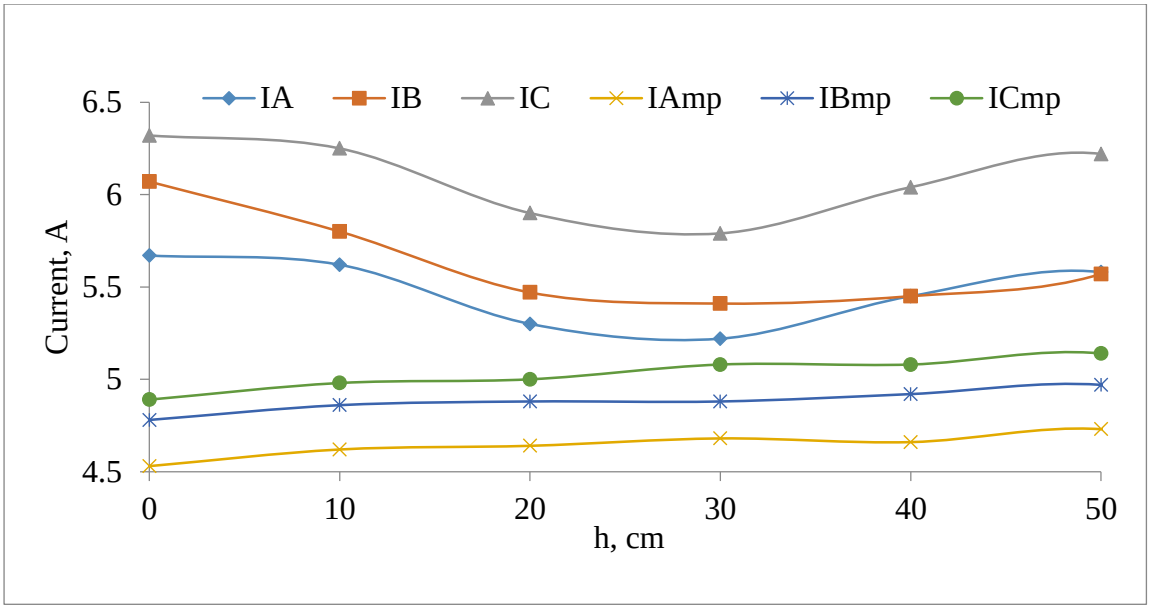

Figure 21: Short circuit current and currents at maximum power for 0-50 cm gap alteration at G=820±10 Wm^{-2}

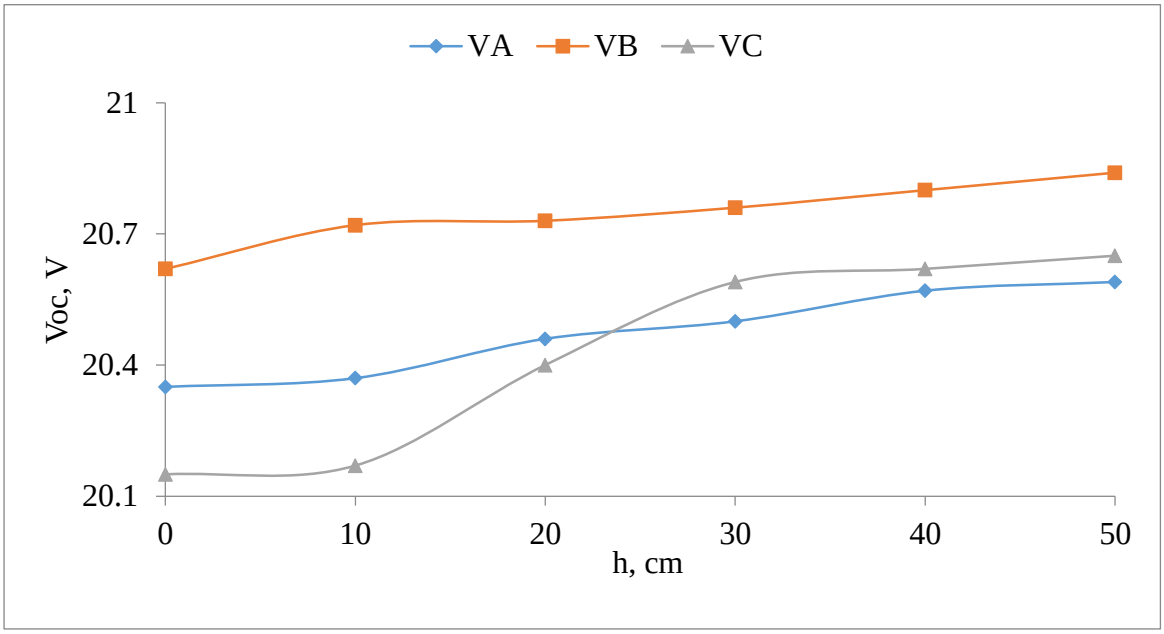

Figure 22: Open circuit voltages for 0-50 cm gap alteration at G=820±10 Wm^{-2}

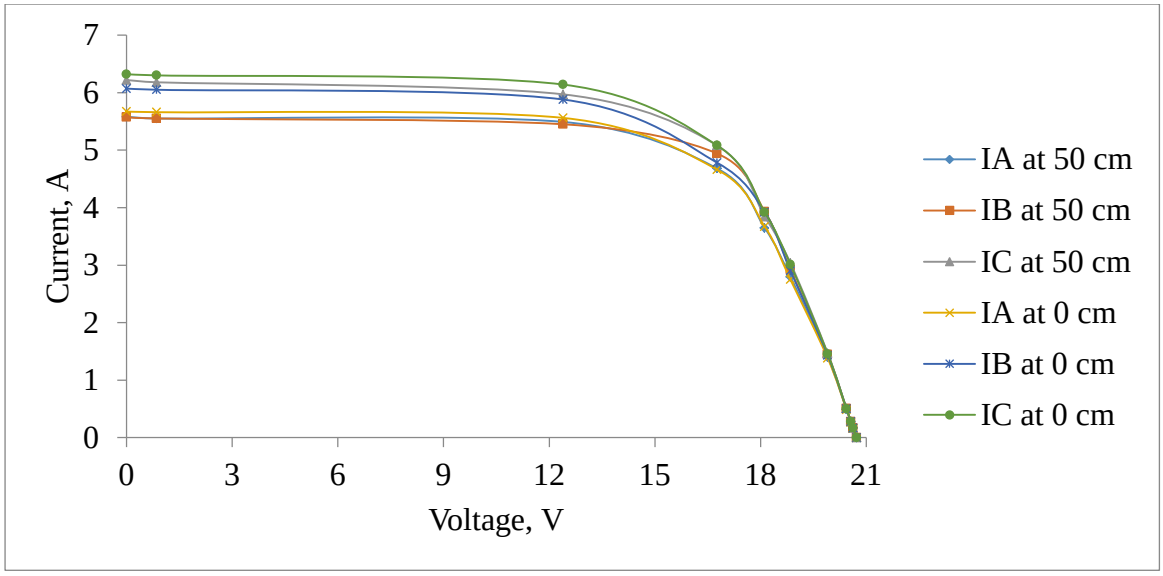

Figure 23: I-V curves at h=0 and50cm at G=820±10 Wm^{-2}

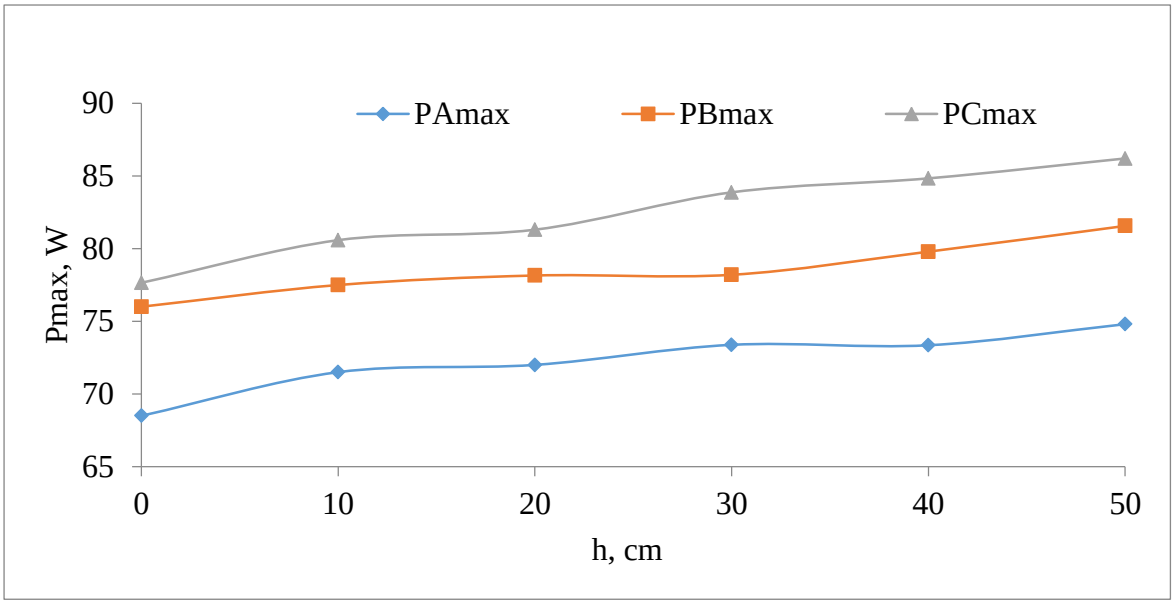

Figure 24: Maximum power solar panels performance for 0 cm-50 cm PV CMS gap alteration at G=820±10 Wm^{-2}

The worst and best scenarios of the solar PV panels' parameters regarding the gap size are found to be in 0 to 50 cm respectively. The efficiency continued to increase in a range of 12.1% to 14.1 % (Fig. 25). Panel A was operating at least efficiency and panel C was working at higher efficiency whist panel B was intermediate when compared to each other. Fill factor (FF) were found to be decreased with increase in PV cell temperature due to decreased PV-CMS gap. Fill factor increased slightly as the gap was enlarged but they were bit less to the manufacturer's (Fig. 26) where FF_B > FF_C > FF_A. Results can be compared to data obtained at standard conditions (Table 2). The panels were generating less

maximum power, open circuit voltage, maximum peak voltage, and maximum peak current during the gap enlargement. Short circuit current generated by panel C was higher to STC (Fig. 21) whilst less was generated by panel A as well as panel B. Though operating temperature reached by the panels were in range specified by the manufacturer (-40 to ~ 85 °C), I-V from 0 to 50 cm gap it indicates that panel C was generating more power compared to others two panels.

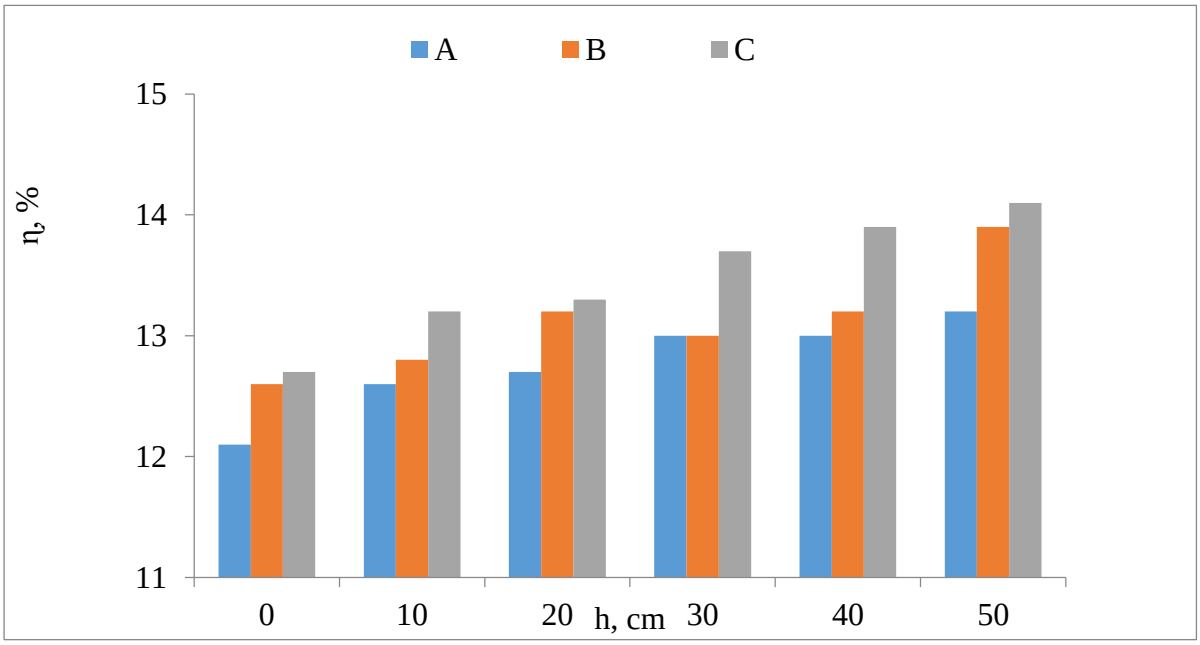

Figure 25: Impact of a gap h between the solar panels and roof on the panels' performance (efficiency) measured outdoor at solar irradiance 820±10 Wm^{-2}

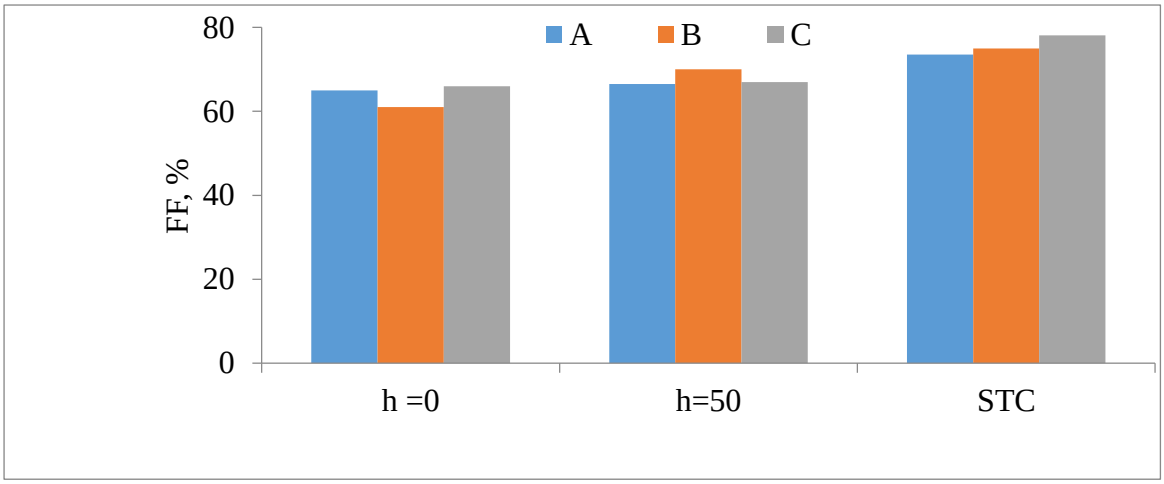

Figure 26: Comparison of panels' fill factors at solar irradiance 820±10 Wm^{-2} and at STC

As seen from previous sections, all panels were of the same capacity and subjected to similar environmental conditions but slightly dissimilarities in output were observed. A small difference in energy collector surface area among the panels can be contributing factor for dissimilarities in outputs. Another possible reasons for output dissimilarities can be due to fact that panels from different regions might have difference in quality of material used, assembling technology used, different testing ideal conditions by the manufacturers, as well as location for application (Sharma and Chandel, 2013). Today there many materials for efficient cell, encapsulate solar cell strings, anti / reflective materials, transparent front glass, low iron glass, or back sheet (plate) (Koehl *et al*., 2011). To conclude this, further research on materials point of view is required.

Again; basing on experimental approach we have obtained that the overall performance of stand-alone SPVP depends on the level of solar irradiance and panel's temperature. For an efficient analysis of stand-alone SPVP systems in terms of technical parameters and performance the short term is indicated. A long-term analysis of stand-alone SPVP system can be used with their embedded components though it can be difficult to study the system components behavior.

4.5 Solar PV panels Matlab simulation

In order to test the validity of the results, the comparisons between the experimental and simulated were carried out. Experimental panels' temperature, electrical parameters and the different irradiance measured during experimental were used as input data to the Matlab function and command codes.

Plotting electrical characteristic curves of the SPVP cells for a certain working irradiance and certain SPVP cell temperature, among them one should fixed (Ishaque *et al*., 2011). The simulated parameters are evaluated during performance using the Equations 3.2, 3.3, 3.4, 3.5, 3.8 3.11, and 3.12 listed in the section 3.4.4. These equations were written in Matlab functions (Appendix 6), and produced Fig. 27 and Fig. 28. The software computes the current (output of the function), using characteristic electrical parameters of the panel, and the variables voltage, panel temperature and solar irradiance (input parameters of the function).

Figure 27 shows simulated I-V curves for the three SPVPs when panels were set at h=0. The three top curves are for G= 820±10 Wm^{-2}, the three curves at the middle are for G= 680±10 Wm^{-2}, and the last three at the bottom stands for G= 480±10 Wm^{-2}. Fig. 28 represents the I-V curves when the panels were set at h= 50 cm and G= 820±10 Wm^{-2}. All curves were found to have similar trend with increased output parameters when the irradiance was improved. Similar observations were reported by Tsai *et al*. (2008), Bonkoungou *et al*. (2013), Park *et al*. (2014) and Bellia *et al*. (2014). The variances of input parameters among panels were factors that contributed a divergent of the I-V curves readouts.

As mentioned in previous sections, short circuit current and open circuit voltage are the supreme significant parameters commonly used for describing the SPVP electrical performance. The aforementioned expressions are implicit and nonlinear; consequently, it is problematic to reach at an investigative result for a set model parameters at a certain irradiance and temperature fluctuations. For this reason, simulations among the SPVPs were done individually due to fact that monitored experimental SPVP parameters were dissimilar. The panels' temperatures were fluctuating in a range of 36 °C to 61 °C depending available solar irradiance whilst the panels' electrical parameters were dissimilar. The situations provided unwanted extra curves though they can be used for predictions for used panels' temperature at different irradiance when needed. To avoid extra curves, the data from simulated individual panels' I-V curves were then combined together, and again, simulated to obtain the I-V curves in single view as displayed in Fig. 27 and Fig. 28.

The nonlinear behavior of PV cell is apparent, that the output current and power of SPVP be influenced by the cell's terminal operating voltage and temperature, and solar irradiance as well. We found that with growth of working cell temperature; short-circuit current increases, whereas the maximum power decreases. The increase in the output current is much less than the decrease in the voltage, the output power decreases at high temperatures. Contrariwise, we observe from Fig. 27 that with increase of solar irradiance, the short-circuit currents of the SPVP increases, and the maximum power output increases as well. The reason is the open circuit voltage is logarithmically reliant on the solar irradiance; nevertheless the short circuit current is directly proportional to the radiant intensity.

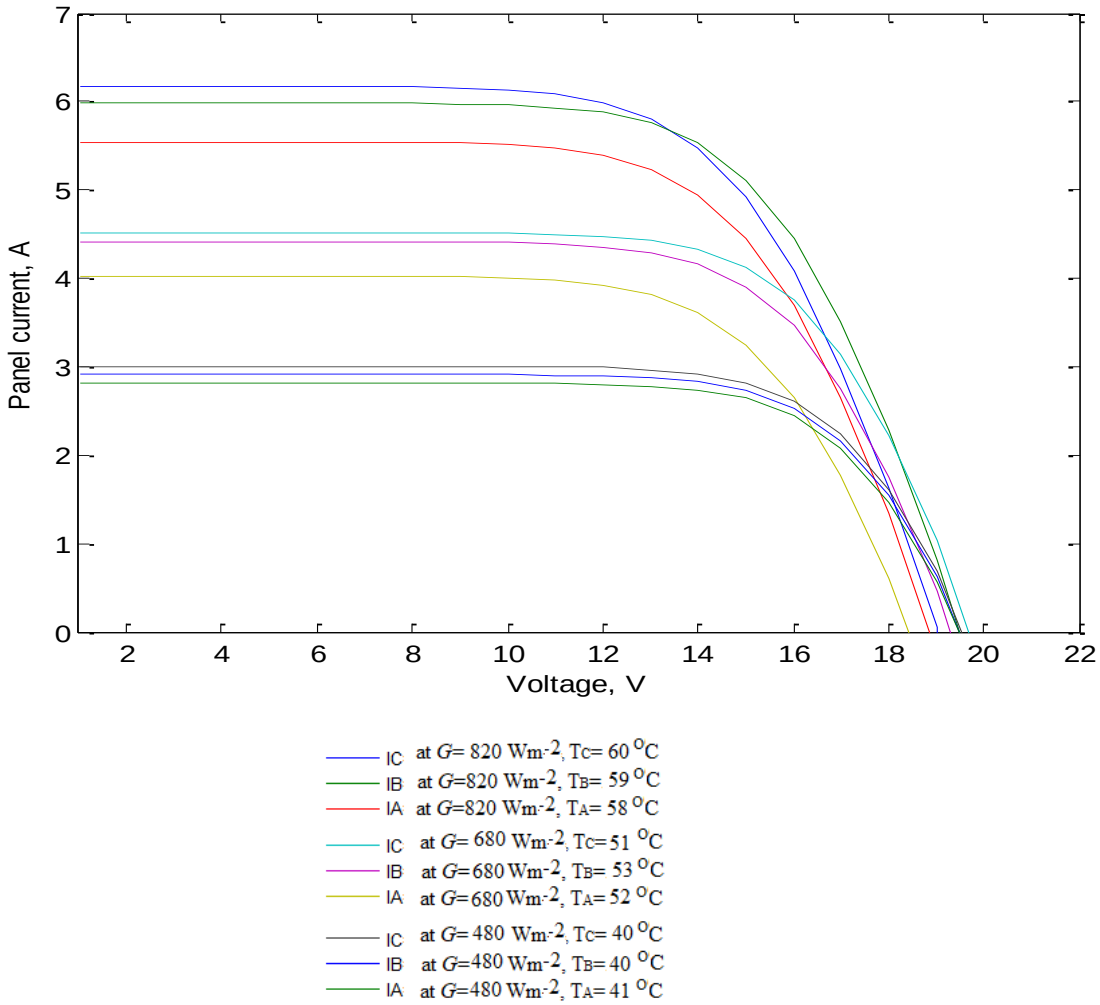

Figure 27: Simulated I-V curves at different irradiance and panel's temperature

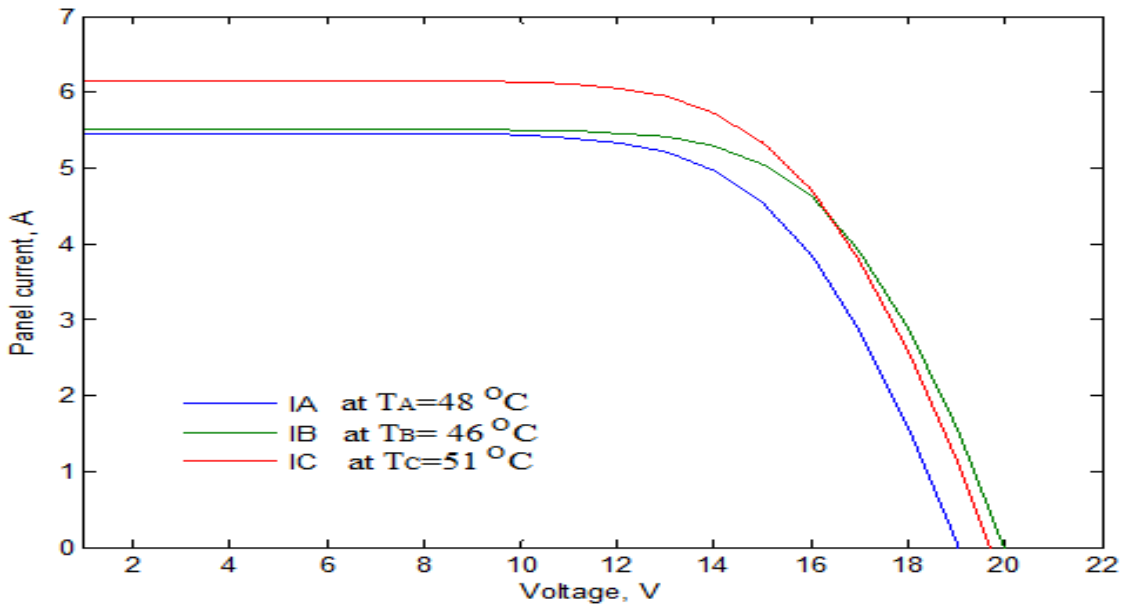

Figure 28: Simulated I-V curves at different irradiance and panel's temperature

The results showed that when compared the experimental results with simulated at h=0 (not plotted due curve clouding); there were insignificant difference between two results. Experimental and simulated I-V curves for each panel at h=50 cm with 820 ±10 Wm^{-2} (Fig. 29) are almost similar. In general, a very good agreement is verified between the experimental and the simulated results hence validating the findings.

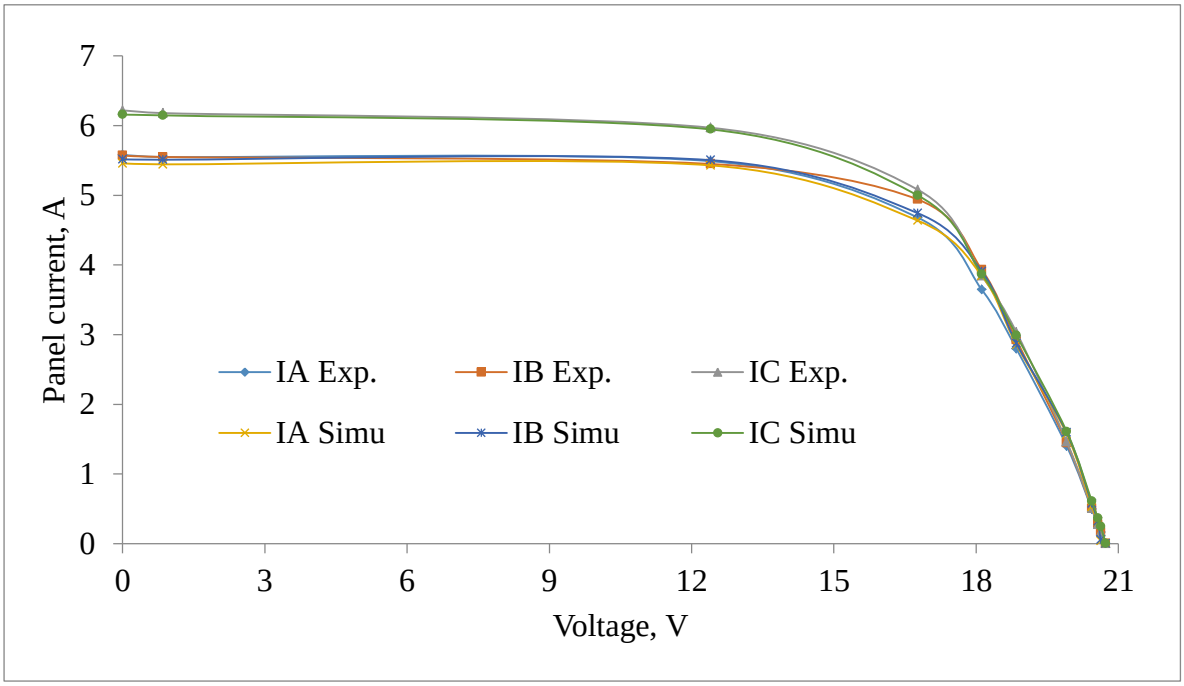

Figure 29: Simulated and experimental I-V curves at G=820±10 Wm^{-2}

Based on experimental and simulation approach we have obtained that the overall performance of stand-alone SPVP depends on the level of solar irradiance and panel's temperature (Chander *et al*., 2015). For an efficient analysis of stand-alone SPVP systems in terms of technical parameters and performance the short term is indicated. A long-term analysis of stand-alone SPVP system can be used with their embedded components though it can be difficult to study the system components behavior. In this study, h (gap size between the solar PV panel and the roof) was not considered in expressions involved in simulations. One can perform a mathematical modeling and simulation study that would involve gap size between the solar PV panel and the roof. Prior, the general knowledge on the CMS materials and its effects on gap variance in relation to simulation are important.

4.6 Effect of partial shading

Experimental performance about shading on SPVP is reported in this section. Fig. 30 and Fig. 31 show the effect of common shadings on short circuit currents and open circuit voltages respectively for the three panels. Panel A and panel C were shaded up to 78% whilst panel B was left un-shaded purposely for making comparison on panels' output current and voltage. It is clear seen that shading up to 22 % provided insignificant change in panels' outputs which probably was due fluctuations in solar irradiance in a range of 930±50 Wm^{-2} during the tests. The short circuit current readouts were in range of ~5.2-5.9 A, ~5.4-6.1 A, and ~5.8-6.75 A for panel A, B, and C respectively. There were noticeable descents for short circuit currents readouts when the shaded cells increased to 58 % and 78 % for panels A and C. The readouts were in range of ~0.8-0.93 A, ~4.98-5.36 A, and ~1.04-1.11 A for panel A, B, and C respectively. A slight plummet on short circuit currents readouts were observed for panel A and C when the panels were 89% and 100% cells shaded whereas for greater fall for $\boldsymbol{I_B}$ was observed.

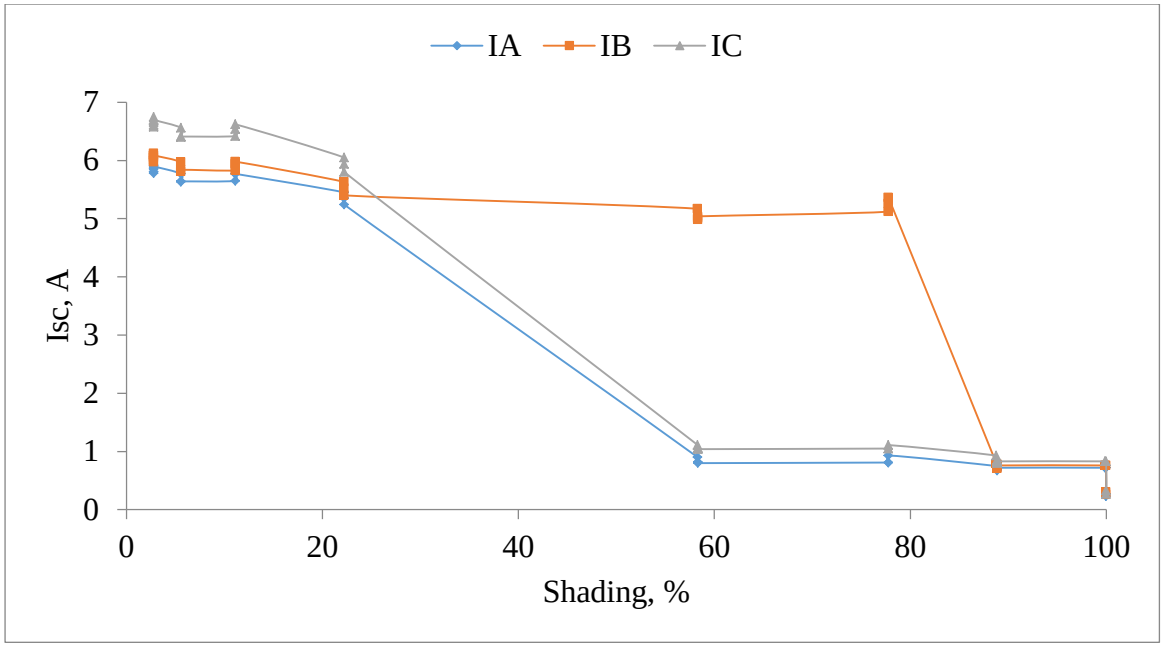

Figure 30: Effect of common shading on short circuit currents for G= 930±50 Wm^{-2} at h=50 cm

Open circuit voltages were observed to decrease when shade percentage was increased. The voltages fluctuated near certain quantities, 21.5 V, 20.7 V, and 20.3 V respectively when the panels shaded up to 58 %, with slight ascent or descent by 0.2 – 0.4 V. Above 58 %, the voltages were reduced to 20.07 V, 19.4 V and 19.3 V with a descending or ascending in a range of 0.3 to 0.5 V. The swings of voltages may be also were due to fluctuation in irradiance that was in range of about 930±50 Wm^{-2}. Under this study, the panels were able to generate a reasonable maximum power which ranged from 111 to 136 watts when shaded up to 22 % whilst slightest ranged between 5 watts to 22 watts when shading was 58% and above.

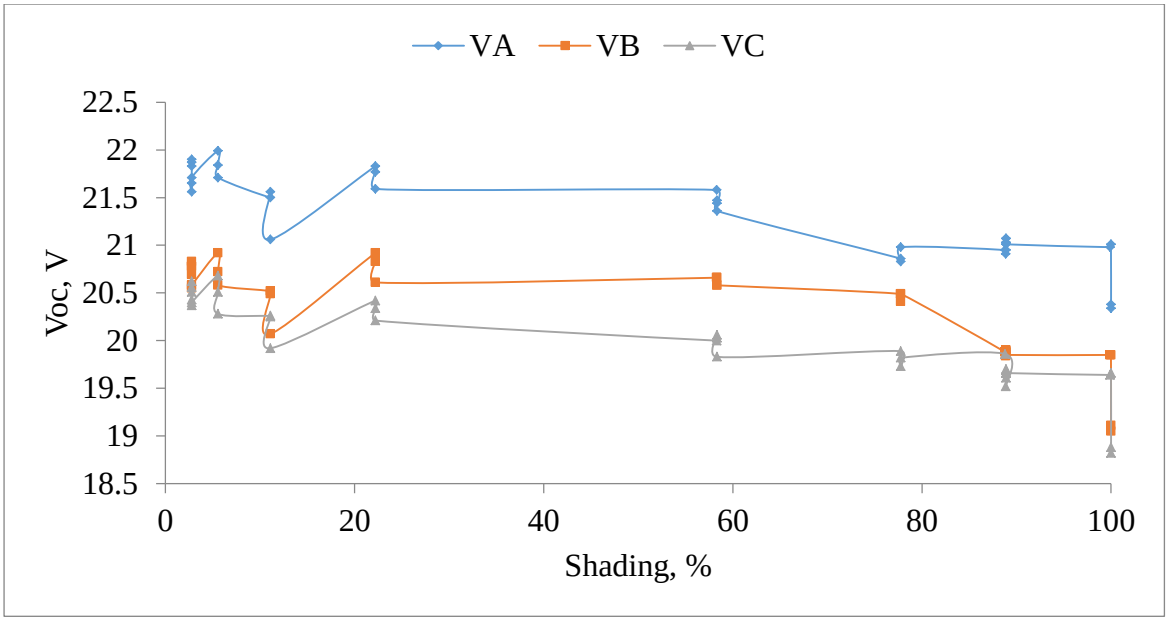

Figure 31: Effect of common shading on open circuit voltage for G=930±50 Wm^{-2} at h=50 cm

For uncommon shading materials, it started by covering one cell at the bottom left side of each panel. Second activity was 6 % which was attained by considering two cells; one cell at the bottom left side of each panel and the other cell at the top-right side of the panel. Third activity was achieved by considering the second test with an addition of four shaded cells at the center of the panels. Lastly; first twenty cells from top to bottom of the two panels were shaded.

The results for uncommon shading in percentage at irradiance G = 400±10 Wm^{-2} are presented in Fig. 32. The highest short circuit currents readouts were 2.59 A, 1.67 A, and 2.96 A for panel A, B, and C respectively when the panels were shaded approximately to 3%. One cell was shaded at the bottom left side of each panel. The readouts were reduced to 0.46 A, 1.2 A, and 2.15 A as least, and 0.57 A, 1.37 A, and 2.45 A as the most readouts when 6% of the panels cells were shaded. It is well seen from panels' readout that with methodology presented by 3 % of shading, panel C was much affected by generating least short circuit current among the panels. When the second method was applied, the situation changed where panel A generated the least short circuit current. Panel C generated no current at 16% shade whilst panels A and B short circuit currents were in range of 0.28-0.44 A. Even at 11 % panel C shade, it continued to generate no current. Below 0.08 A and 0.17

A were the short circuit current readouts for panels A and B when 56 percent shading were considered.

Every panel showed a significant difference in short circuit current readout when a particular shade method was applied. To conclude on this, the electrical connections of the PVs' cells among the panel may be are not similar. Therefore, shading any cell to your panel could reduce system performance.

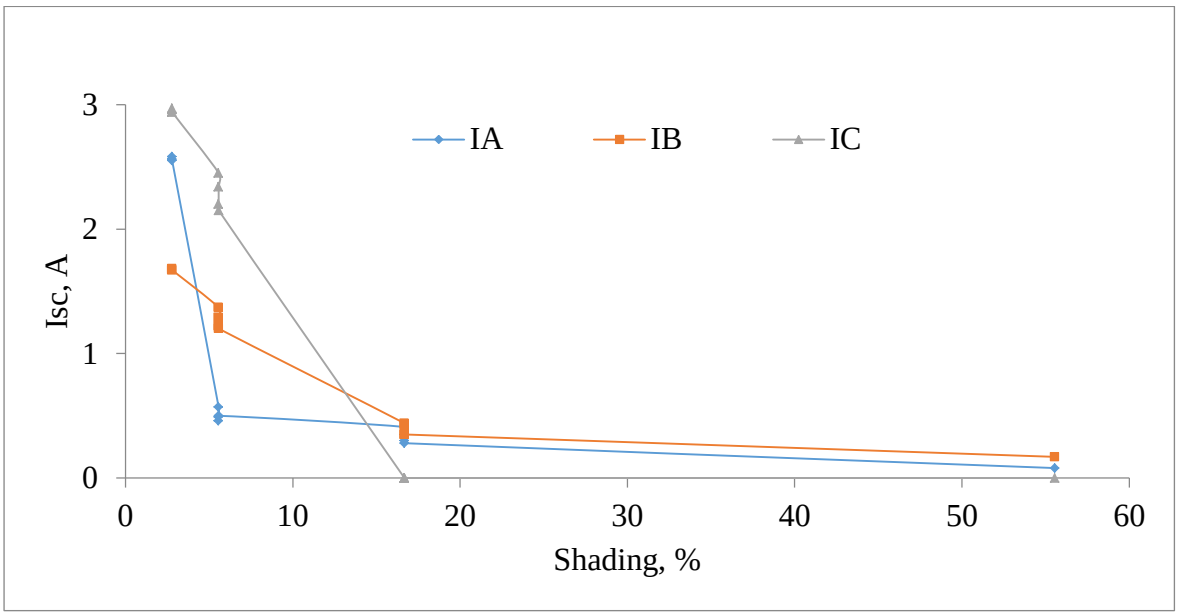

Figure 32: Effect of uncommon shading on short circuit current at 400±10 Wm^{-2} at h=50cm

When compared the present results with those obtained at 480 ± 10 Wm^{-2} and 820 ±10 Wm^{-2} performance tests, it is clear that all panels were affected by shading. The study concur with previous theoretical studies made by Ramabadran and Mathur (2009), Shaiek *et al*. (2013), Fialho *et al*. (2014), Kivaisi (2000). Ramabadran and Mathur (2009) pointed out that the outputs are reduced due to less energy reaching the PV cells and the increased losses in shaded PV cells. Shaiek *et al*. (2013) reported that the outputs are resulting in multiple peaks if the panel does not receive uniform insolation caused either by passing clouds or neighboring building, towers, trees, telephone poles over the panel surface. Fialho *et al*. (2014) pointed out that even small shadows on SPVP can noticeably affect the energy yield. Karatepe *et al*. (2007) also point out that under shading conditions, higher short circuit current are generated in shaded cells and creates worse situation to the panel that can cause cracking for the soldered parts of the cell.

It was observed that with non-uniform shading (tree / plant leaves), electrical parameters readouts and panel temperature were affected depending on how far the shading is from the panel and leaves concentration towards shaded cells. Panels' temperature slightly continued falling under shading condition subject to coverage and it was abruptly increased after a short time of a shading removal. The opaque shading (front touched) stopped to generate current even when it was shaded only at the center (eleven percent). Uniform shading (pole, house or bird droppings depending on coverage on panels) brings to your system with less or no power generated. The shading on SPVP causes energy loss and also more nonlinearity on the electrical characteristics curves (Fialho *et al*., 2014). Mounting PV modules at free shadowing area should be given in need of attention which accords to Kivaisi (2000) PV modules installation recommendation.

CHAPTER FIVE

CONCLUSION AND RECOMMENDATIONS

5.1 Summary of the study

The study aimed at analysing the performance analysis of standalone polycrystalline silicon solar PV panel. The objectives of this research were to evaluate the performance of standalone polycrystalline silicon SPVP from different manufactures on natural air passive cooling by varying gap between pitched CMS roof and panel, to assess the simulation performance of standalone SPVP under different working conditions, and to understand the effects of shading on performance of SPVPs.

The study employed experimental as well as theoretical approach so as to get a holistic understanding polycrystalline silicon SPVP performance. The experimental setup was composed of three polycrystalline silicon SPVPs from three different manufacturers. The SPVPs were mounted on the same structure with same equipment and accessories setups. It should be noted that, the study did not consider all the aspects of exact building but done at a platform structures serving as house roof. Prior to carry outdoor experimental work, the system settings and constant readouts of outdoor environmental parameters such as solar irradiance, ambient temperature, relative humidity, and wind speed were important to keep. Most of the faced challenges were fluctuations of outdoor readout parameters which also are the real situations that the panels face when are outdoor mounted. Experimental performance was carried out at irradiance of 480±10 Wm^{-2}, 680± 10 Wm^{-2}, and 820±10 Wm^{-2}, whilst the gap between the panel and CMS was varied from 0 to 50 cm. The variable experimental data were used in theoretical study as an inputs in Matlab function. Common shadings were done following ~3 to 100 % at irradiance of 930±50 Wm^{-2} whereas uncommon shading was done from ~3 to ~16 % for all panels at of 400±10 Wm^{-2}, above 16 % of shade only panel A and B were considered.

5.2 Conclusion

Main findings were the CMS effects on solar PV panel performance. Short circuit and open circuit voltage were the supreme significant parameters commonly used for describing the SPVP electrical performance. The power outputs were reduced by 5%-11% when the solar PV panel was mounted directly on the roof compared to 50 cm gap.

Moreover solar panel temperature exceeded the ambient one by 28 - 35 degrees that was much higher than usually accepted about 15 °C for standalone PV system. Apparently the PV extra heat originated from roof vicinity; in-spite the roof temperature appeared lower by ~5-18 °C than that of a panel. A gap between the roof surface and panel was helpful to reduce extra heating solar panel and increase the power; the large size of the gap favored better performance of solar PV panel. Therefore, PVs mounted at least 50 cm or more above the CMS could operate within the nominal operating cell temperature and will generate good power.

Simultaneous monitoring of the three polycrystalline silicon panels' performance revealed rather synchronous behavior of temperatures and electrical parameters regarding change in irradiance or gap size that confirms reliability of the results obtained. Experimental and simulated electrical characteristics curves evolution found to have similar trend though there were some difference in readouts at higher solar irradiance with higher SPVP temperature.

Shading caused less energy harvested due least current generated by the PV generator. Though it were observed the dissimilarities in outputs when uncommon shade were applied, but still even small shade can bring your system with no power, and if the power is generated, the output electrical parameter become more nonlinear.

5.3 Recommendations

Proper performance of the SPVP mounted on the roof, the following recommendations were observed from this work.

i. Mounting PV modules directly on CMS roof should be avoided and always the gap should be provided at least 10 cm or above. The more the gap, the mounting structure should be strongly fixed to withstand gale and system steadiness.
ii. During planning for mounting the SPVM; it is important to minimize the factors that are likely to cause module shading. Selecting the best place for mounting panels enables to recognize misbehaving issues of the system early in the process when it is well monitored.
iii. People may fail to realize the effect but even a small amount of shading can have effect on the SPVP outputs. Removal of nearby trees, leaves, bird droppings, and

other airborne objects ensures sufficient energy production guaranteeing finest system owner rebate.

iv. It is a good practice to have routine cleaning on the front surface panel to avoid reduced module efficiency. For safety reasons, the uses of metal or harsh objects for removing coated materials are to be avoided. Scratching the glass on a SPVP will cast shadows for which local hot spot occurs. The use of appropriate safety equipment and training to access the rooftop is necessary. Soft brushes, squeegee with a plastic blade on one side or cloth covered sponge are useful for panel cleaning.

v. A similar study can be performed to investigate the influence on different roofing materials or one can develop a PV temperature estimation model for different types of roofing materials.

vi. Once again, one can perform a simulation study that would involve gap size between the solar PV panel and the roof in Matlab coding. Prior carrying the study, the knowledge on materials made the CMS and its effects on gap variance in relation to PV simulation is important.

vii. Comparable study for monocrystalline, polycrystalline, and amorphous of the same size can be conducted.

REFERENCES

Ahlborg, H. and Hammar, L. (2014). Drivers and barriers to rural electrification in tanzania and mozambique - grid-extension, off-grid, and renewable energy technologies. *Renewable Energy*. *61*, 117–124.

Arjyadhara, P., Ali, S.M. and Chitralekha, J. (2013). Analysis of Solar PV cell Performance with Changing Irradiance and Temperature. *International Journal Of Engineering And Computer Science*. *2*(1), 214–220.

Armstrong, S. and Hurley, W. G. (2010). A thermal model for photovoltaic panels under varying atmospheric conditions. *Applied Thermal Engineering*. *30*(11–12), 1488–1495.

Bellia, H., Youcef, R. and Fatima, M. (2014). A detailed modeling of photovoltaic module using MatLab. *NRIAG Journal of Astronomy and Geophysics*. *3*(1), 53–61.

Bergamasco, L. and Asinari, P. (2011). Scalable methodology for the photovoltaic solar energy potential assessment based on available roof surface area : Application to Piedmont Region (Italy). *Solar Energy*. *85*(5), 1041–1055.

Bonkoungou, D., Koalaga, Z. and Njomo, D. (2013). Modelling and simulation of photvolotaic module considering single-diode equivalent circuit model in MatLab Modelling and Simulation of photovoltaic module considering single-diode equivalent circuit model in MatLab. *International Journal of Emerging Technology and Advanced Engineering*. *3*(3).

Chander, S., Purohit, A., Sharma, A., Nehra, S. P. and Dhaka, M. S. (2015). A study on photovoltaic parameters of mono-crystalline silicon solar cell with cell temperature. *Energy Reports*. *1*, 104–109.

Chikate, B. V. and Sadawarte, Y. (2015). The Factors Affecting the Performance of Solar Cell. In *International Journal of Computer Applications. (0975 – 8887)* (pp. 1–5).

Darwish, Z. A., Kazim, H. A., Sopian, K., Alghoul, M. A. and Chaichan, M. T. (2013). Impact of Some Environmental Variables with Dust on Solar Photovoltaic (PV) Performance: Review and Research Status. *International Journal of Energy and Environment*. *7*(4), 152–159.

Deichmann, U., Meisner, C., Murray, S. and Wheeler, D. (2011). The economics of renewable energy expansion in rural Sub-Saharan Africa. *Energy Policy*. *39*(1), 215–227.

Demirbas, A. (2005). Potential applications of renewable energy sources, biomass combustion problems in boiler power systems and combustion related environmental issues. *Progress in Energy and Combustion Science*. *31*(2), 171–192.

Dominguez, A., Kleissl, J. and Luvall, J. C. (2011). Effects of solar photovoltaic panels on roof heat transfer. *Solar Energy*. *85*(9), 2244–2255.

Dubey, S., Sarvaiya, J. N. and Seshadri, B. (2013). Temperature dependent photovoltaic (PV) efficiency and its effect on PV production in the world - A review. *Energy Procedia*. *33*, 311–321.

Ellabban, O. and Blaabjerg, F. (2014). Renewable energy resources : Current status , future prospects and their enabling technology. *Renewable and Sustainable Energy Reviews*. *39*, 748–764.

Elminir, H. K., Ghitas, A. E., Hamid, R. H., El-Hussainy, F., Beheary, M. M. and Abdel-Moneim, K. M. (2006). Effect of dust on the transparent cover of solar collectors. *Energy Conversion and Management*. *47*(18–19), 3192–3203.

Fara, L. and Craciunescu, D. (2017). Output Analysis of Stand-Alone PV Systems : Modeling, Simulation and Control. *Energy Procedia*. *112*, 595–605.

Fesharaki, V. J., Dehghani, M., Fesharaki, J. J. and Tavasoli, H. (2011). The Effect of Temperature on Photovoltaic Cell Efficiency. *Proceeding of the 1st International Conference on Emerging Trends in Energy Conservation-ETEC*. 20–21.

Fialho, L., Melicio, R., Mendes, V. M. F., Figueiredo, J. and Collares-pereira, M. (2014). Effect of Shading on Series Solar Modules : Simulation and Experimental Results. *Procedia Technology*. *17*, 295–302.

Gooding, J., Crook, R. and Tomlin, A. S. (2015). Modelling of roof geometries from low-resolution LiDAR data for city-scale solar energy applications using a neighbouring buildings method. *Applied Energy*. *148*, 93–104.

Grubišić-Čabo, F., Nižetić, S. and Marco, T. G. (2016). Photovoltaic Panels : a Review of the Cooling Techniques. *Transactions of Famena XL*. *1*(1), 63–74.

Honsberg, C. and Bowden, S. (2014). Nominal Operating Cell Temperature. Retrieved March 5, 2018, from http://www.pveducation.org/pvcdrom/modules/nominal-operating-cell-temperature

Honsberg, C. and Bowden, S. (2016). Heat Loss in PV Modules | PV Education. Retrieved March 6, 2018, from http://www.pveducation.org/pvcdrom/modules/heat-loss-in-pv-modules

Ishaque, K., Salam, Z. and Teheri, H. (2011). Accurate MatLab Simulink PV System Simulator Based on a Two-Diode model. *Journal of Power Electronics*. *11*(2).

Jacobson, A. (2007). Connective Power : Solar Electrification and Social Change in Kenya. *World Development*. *35*(1), 144–162.

Jacobson, M. Z. and Jadhav, V. (2018). World estimates of PV optimal tilt angles and ratios of sunlight incident upon tilted and tracked PV panels relative to horizontal panels. *Solar Energy*. *169*, 55–66.

Kaldellis, J. K., Kapsali, M. and Kavadias, K. A. (2014). Temperature and wind speed impact on the ef fi ciency of PV installations . Experience obtained from outdoor measurements in Greece. *Renewable Energy*. *66*, 612–624.

Karatepe, E., Boztepe, M. and Metin, C. (2007). Development of a suitable model for characterizing photovoltaic arrays with shaded solar cells. *Solar Energy*. *81*, 977–992.

Khan, M., Ko, B., Nyari, E. A., Park, S. E. P. and Kim, H.J. (2017). Performance Evaluation of Photovoltaic Solar System with Different Cooling Methods and a Bi-Reflector Comparative Analysis. *Energies*. *10*(826), 23.

Khare, V., Nema, S. and Baredar, P. (2013). Status of solar wind renewable energy in India $. *Renewable and Sustainable Energy Reviews*. *27*, 1–10.

Kihwele, S., Hur, K. and Kyaruzi, A. (2012). Visions, Scenarios and Action Plans Towards Next Generation Tanzania Power System. *Energies*. 3908–3927.

Kivaisi, R. T. (2000). Installation and use of a 3 kW p PV plant at Umbuji village in Zanzibar. *Renewable Energy*. *19*, 457–472.

Koehl, M., Heck, M., Wiesmeier, S. and Wirth, J. (2011). Solar Energy Materials and Solar Cells Modeling of the nominal operating cell temperature based on outdoor weathering. *Solar Energy Materials and Solar Cells*. *95*(7), 1638–1646.

Kulworawanichpong, T. and Mwambeleko, J. J. (2015). Design and costing of a stand-alone solar photovoltaic system for a Tanzanian rural household. *Sustainable Energy Technologies and Assessments*. *12*, 53–59.

Lee, Y. and Tay, A. A. O. (2012). Energy Procedia Finite Element Thermal Analysis of a Solar Photovoltaic Module. *Energy Procedia*. *15*, 413–420.

Mani, M. and Pillai, R. (2010). Impact of dust on solar photovoltaic (PV) performance : Research status , challenges and recommendations. *Renewable and Sustainable Energy Reviews*. *14*(9), 3124–3131.

Mattei, M., Notton, G., Cristofari, C., Muselli, M. and Poggi, P. (2006). Calculation of the polycrystalline PV module temperature using a simple method of energy balance. *Renewable Energy*. *31*, 553–567.

Mekhilef, S., Saidur, R. and Kamalisarvestani, M. (2012). Effect of dust, humidity and air velocity on efficiency of photovoltaic cells. *Renewable and Sustainable Energy Reviews*. *16*(5), 2920–2925.

Mellit, A., Kalogirou, S. A., Shaari, S., Salhi, H. and Hadj, A. A. (2008). Methodology for predicting sequences of mean monthly clearness index and daily solar radiation data in remote areas: Application for sizing a stand-alone PV system. *Renewable Energy*. *33*(7), 1570–1590.

Meral, M. E. and Diner, F. (2011). A review of the factors affecting operation and efficiency of photovoltaic based electricity generation systems. *Renewable and Sustainable Energy Reviews*. *15*(5), 2176–2184.

Mohammed, S. S. (2011). Modeling and Simulation of Photovoltaic module using MatLab / Simulink. *International Journal of Chemical and Environmental Engineering Modeling*.

2(5).

Muzathik, A. M. (2014). Photovoltaic Modules Operating Temperature Estimation Using a Simple Correlation. *International Journal of Energy Engineering*. *4*, 151–158.

Nyari, E. A., Pogrebnaya, T. and Wilson, L. (2015). Energy Sector and Solar Energy Potential in Tanzania. *International Journal of Emerging Technologies and Engineering*. *2*(9), 2348–8050.

Ondraczek, J. (2013). The sun rises in the east (of Africa): A comparison of the development and status of solar energy markets in Kenya and Tanzania. *Energy Policy*. *56*, 407–417.

Panwar, N. L., Kaushik, S. C. and Kothari, S. (2011). Role of renewable energy sources in environmental protection : A review. *Renewable and Sustainable Energy Reviews*. *15*(3), 1513–1524.

Parida, B., Iniyan, S. and Goic, R. (2011). A review of solar photovoltaic technologies. *Renewable and Sustainable Energy Reviews*. *15*(3), 1625–1636.

Park, J., Kim, H., Cho, Y. and Shin, C. (2014). Simple Modeling and Simulation of Photovoltaic Panels Using Matlab / Simulink Modeling of Photovoltaic Module. *Advanced Science and Technology Letters*. *73*, 147–155.

Patel, H. and Agarwal, V. (2008). MatLab-Based Modeling to Study the Effects of Partial Shading on PV Array Characteristics. *IEEE Transactions on Energy Conversion*. *23*(1), 302–310.

Ramabadran, R. and Mathur, B. L. (2009). Impact of partial shading on solar PV module containing series connected cells. *International Journal of Recent Trends in Engineering*. *2*.

Salmi, T., Bouzguenda, M., Gastli, A. and Masmoudi, A. (2012). MatLab / Simulink Based Modelling of Solar Photovoltaic Cell. *International Journal of Renewable Energy Research*. *2*(2).

Schwingshackl, C., Petitta, M., Wagner, J. E., Belluardo, G. and Moser, D. (2013). Wind effect on PV module temperature : Analysis of different techniques for an accurate estimation. *Energy Procedia*. *40*, 77–86.

Shaiek, Y., Smida, M. B., Sakly, A. and Mimouni, M. F. (2013). Comparison between conventional methods and GA approach for maximum power point tracking of shaded solar PV generators. *Solar Energy*. *90*, 107–122.

Sharma, V. and Chandel, S. S. (2013). Performance and degradation analysis for long term reliability of solar photovoltaic systems: A review. *Renewable and Sustainable Energy Reviews*. *27*, 753–767.

Sheya, M. S. and Mushi, S. J. S. (2000). The state of renewable energy harnessing in Tanzania. *Applied Energy*. *65*(1–4), 257–271.

Sirisamphanwong, C. and Ketjoy, N. (2012). Impact of spectral irradiance distribution on the outdoor performance of photovoltaic system under Thai climatic conditions. *Renewable Energy*. *38*(1), 69–74.

Skoplaki, E. and Palyvos, J. A. (2009). On the temperature dependence of photovoltaic module electrical performance : A review of efficiency / power correlations. *Solar Energy*. *83*(5), 614–624.

Solangi, K. H., Islam, M. R., Saidur, R., Rahim, N. A. and Fayaz, H. (2011). A review on global solar energy policy. *Renewable and Sustainable Energy Reviews*. *15*(4), 2149–2163.

Stathopoulos, T. (2003). Wind loads on low buildings: In the wake of Alan Davenport's contributions. *Journal of Wind Engineering and Industrial Aerodynamics*. *91*(12–15), 1565–1585.

Szabo´, S., B'odis, K., Huld, T. and Moner, G. M. (2011). Energy solutions in rural Africa : mapping electrification costs of distributed solar and diesel generation versus grid extension. *Environmental Research Letters*.

Touati, F. A., Al-hitmi, M. A. and Bouchech, H. J. (2012). Study of the Effects of Dust, Relative Humidity, and Temperature on Solar PV Performance in Doha : Comparison Between Monocrystalline and Amorphous PVS. *International Journal of Green Energy*. 37–41.

Tsai, H., Tu, C. and Su, Y. (2008). Development of Generalized Photovoltaic Model Using

MatLab / Simulink. *Proceedings of the World Congress on Engineering and Computer Science 2008 WCECS 2008, October 22 - 24, 2008. San Francisco, USA*, 6.

Tyagi, V. V., Rahim, N. A. A., Rahim, N. A. and Selvaraj, J. A. L. (2013). Progress in solar PV technology : Research and achievement. *Renewable and Sustainable Energy Reviews*. *20*, 443–461.

Yadav, A. K. and Chandel, S. S. (2013). Tilt angle optimization to maximize incident solar radiation: A review. *Renewable and Sustainable Energy Reviews*. *23*, 503–513.

APPENDICES

Appendix 1: Data acquisition system input codes

```
#include <LiquidCrystal.h>
#include <dht.h>
#include <SPI.h>
#include <SD.h>
#include <Wire.h>
#include <TimeLib.h>
#include <DS1307RTC.h>
dht DHT;
#define chipSelect 53
#define LED 12
#define CVMode 7
#define LDR A14
#define Dht A13
#define LM35_1 A8
#define LM35_2 A9
#define LM35_3 A10
#define LM35_Roof A12
#define Voltmeter1 A2
#define Voltmeter2 A1
#define Voltmeter3 A0
#define Ammeter1 A6
#define Ammeter2 A7
#define Ammeter3 A11
#define Anemometer 2
#define Ratio1V 0.030452859
#define Ratio2V 0.028189241
#define Ratio3V 0.028131674
#define Ratio1T 0.556080896
#define Ratio2T 0.554687209
#define Ratio3T 0.526315789
#define Ratio4T 0.514285714
#define RatioAT 1.176470588
#define RatioRH 1.328846154
#define Ratio1C 1.01799295555
#define Ratio2C 0.99499828192
#define Ratio3C 1.03273137697


//Initialize the library with the numbers of the interface pins
LiquidCrystal lcd(16, 17, 18, 19,15,14);

float
Total=0,VPanel1=0,VPanel2=0,VPanel3=0,CPanel1=0,CPanel2=0,v2=0,Temp=
0,Hum=0,
CPanel3=0,Temp1=0,Temp2=0,Temp3=0,TempRoof=0,Voltage=0;
char i=0,sClr=0,sCrn=0,Tx=0,Rx='0';

tmElements_t tm;
```

```
//Setup function
void setup() {
//Configurations
   pinMode(Voltmeter1,INPUT);   pinMode(Voltmeter2,INPUT);
   pinMode(Voltmeter3,INPUT);   pinMode(Ammeter1,INPUT);
   pinMode(Ammeter2,INPUT);     pinMode(Ammeter3,INPUT);
   pinMode(LDR,INPUT);          pinMode(LM35_1,INPUT);
   pinMode(LM35_2,INPUT);       pinMode(LM35_3,INPUT);
   pinMode(LM35_Roof,INPUT);    pinMode(LED,OUTPUT);
   pinMode(CVMode,OUTPUT);   pinMode(Anemometer,INPUT);
   digitalWrite(CVMode,LOW);
   lcd.begin(20, 4);
   Serial.begin(9600);
   if (!SD.begin(chipSelect))
      Serial.println("Card failed, or not present");
   else
      Serial.println("card initialized."); //Configurations

//Initiallization
   lcd.setCursor(0, 0);
   lcd.print("Booting..");
   lcd.setCursor(0, 1);
   for(i=0;i<20;i++){
     lcd.print('.');
     digitalWrite(LED,HIGH);
     delay(200);
     digitalWrite(LED,LOW);
     delay(200);
   }digitalWrite(LED,HIGH);
   lcd.setCursor(2,2);
   lcd.print("**WELCOME TO!**");
   lcd.setCursor(0,3);
   lcd.print("*NICKSON'S RESEARCH*");
}//Setup function
//Main function
void loop() {
//********Sensor reading and quantization ********
//Temperature1
   for(i=0;i<100;i++){
      Total+=analogRead(LM35_1);
      delay(2);
   }Temp1=Total/100*Ratio1T;
   Total=0;
//Temperature2
   for(i=0;i<100;i++){
      Total+=analogRead(LM35_2);
      delay(2);
   }Temp2=Total/100*Ratio2T;
   Total=0;
//Temperature3
   for(i=0;i<100;i++){
      Total+=analogRead(LM35_3);
      delay(2);
   }Temp3=Total/100*Ratio3T;
   Total=0;
//TemperatureRoof
```

```
    for(i=0;i<100;i++){
       Total+=analogRead(LM35_Roof);
       delay(2);
    }TempRoof=Total/100*Ratio4T;
    Total=0;
 //Time/Dht
    int chk = DHT.read11(Dht);
    Temp=DHT.temperature*RatioAT;
    Hum=DHT.humidity*RatioRH;
 //********Sensor reading and quantization ********
 //********Display ********
    if(sCrn>4){
       if(sClr!=1)
          lcd.clear();
       sClr=1;
       Time();
       lcd.setCursor(4,1);
       lcd.print("SOLAR PANELS");
       lcd.setCursor(0,2);
       lcd.print("_PARAMETER ANALYSER_");
       lcd.setCursor(0,3);
       lcd.print("Nelson Mandela Inst.");
    }else{
       if(sClr!=2)
          lcd.clear();
       sClr=2;
       Time();
       lcd.setCursor(0,1);
       lcd.print("T1:");   lcd.print(Temp1,1);
lcd.print(char(0xDF));   lcd.print('C');
       lcd.setCursor(11,1);
       lcd.print("T2:");   lcd.print(Temp2,1);
lcd.print(char(0xDF));   lcd.print('C');
       lcd.setCursor(0,2);
       lcd.print("T3:");   lcd.print(Temp3,1);
lcd.print(char(0xDF));   lcd.print('C');
       lcd.setCursor(11,2);
       lcd.print("RT:");   lcd.print(TempRoof,1);
lcd.print(char(0xDF));   lcd.print('C');
       lcd.setCursor(0,3);
       lcd.print("AT:");   lcd.print(Temp,1);
lcd.print(char(0xDF));   lcd.print('C');
       lcd.setCursor(11,3);
       lcd.print("Rh:");   lcd.print(Hum,1);   lcd.print('%');
    }sCrn++;
    if(sCrn>5)
       sCrn=0; delay(800); //********Display ********
 //******** dataFile Display ********
    Tx++;
    if(Tx>60){
       VCFunction();
       digitalWrite(CVMode,LOW);
       Serial.print("Date/Time: ");
       Serial.print(tm.Day);   Serial.print('/');
Serial.print(tm.Month);  Serial.print('/');
Serial.print(tmYearToCalendar(tm.Year));
```

```
        Serial.print("   ");   Serial.print(tm.Hour);
Serial.print(':');   Serial.println(tm.Minute);
        Serial.println("*VOLTAGE*");
        Serial.print("P1: ");   Serial.print(VPanel1,2);
Serial.println('V');
        Serial.print("P2: ");   Serial.print(VPanel2,2);
Serial.println('V');
        Serial.print("P3: ");   Serial.print(VPanel3,2);
Serial.println('V');
        Serial.println();
        Serial.println("*CURRENT*");
        Serial.print("P1: ");   Serial.print(CPanel1,2);
Serial.println('A');
        Serial.print("P2: ");   Serial.print(CPanel2,2);
Serial.println('A');
        Serial.print("P3: ");   Serial.print(CPanel3,2);
Serial.println('A');
        Serial.println();
        Serial.println("*TEMPERATURE*");
        Serial.print("RT: ");    Serial.print(TempRoof,1);
Serial.println('C');
        Serial.print("AT: ");   Serial.print(DHT.temperature,1);
Serial.println('C');
        Serial.print("P1: ");   Serial.print(Temp1,2);
Serial.println('C');
        Serial.print("P2: ");   Serial.print(Temp2,2);
Serial.println('C');
        Serial.print("P3: ");   Serial.print(Temp3,2);
Serial.println('C');
        Serial.println();
        Serial.println("*ENVIRONMENT*");
        Serial.print("Rh: ");   Serial.print(DHT.humidity,1);
Serial.println('%');
        Serial.println();
        File dataFile = SD.open("Data.txt", FILE_WRITE);
        if (dataFile) {
           dataFile.print("Date/Time: ");
           dataFile.print(tm.Day);   dataFile.print('/');
dataFile.print(tm.Month);  dataFile.print('/');
dataFile.print(tmYearToCalendar(tm.Year));
           dataFile.print("   ");   dataFile.print(tm.Hour);
dataFile.print(':');   dataFile.println(tm.Minute);
           dataFile.println("*VOLTAGE*");
           dataFile.print("P1: ");   dataFile.print(VPanel1,2);
dataFile.println('V');
           dataFile.print("P2: ");   dataFile.print(VPanel2,2);
dataFile.println('V');
           dataFile.print("P3: ");   dataFile.print(VPanel3,2);
dataFile.println('V');
           dataFile.println();
           dataFile.println("*CURRENT*");
           dataFile.print("P1: ");   dataFile.print(CPanel1,2);
dataFile.println('A');
           dataFile.print("P2: ");   dataFile.print(CPanel2,2);
dataFile.println('A');
```

```
          dataFile.print("P3: ");   dataFile.print(CPanel3,2);
dataFile.println('A');
          dataFile.println();
          dataFile.println("*TEMPERATURE*");
          dataFile.print("RT: ");    dataFile.print(TempRoof,1);
dataFile.println('C');
          dataFile.print("AT: ");
dataFile.print(DHT.temperature,1);   dataFile.println('C');
          dataFile.print("P1: ");   dataFile.print(Temp1,2);
dataFile.println('C');
          dataFile.print("P2: ");   dataFile.print(Temp2,2);
dataFile.println('C');
          dataFile.print("P3: ");   dataFile.print(Temp3,2);
dataFile.println('C');
          dataFile.println();
          dataFile.println("*ENVIRONMENT*");
          dataFile.print("Rh: ");   dataFile.print(DHT.humidity,1);
dataFile.println('%');
          dataFile.close();
       }else
          Serial.println("error opening Data.txt");
       Tx=0;   Serial.println();    Serial.println(); delay(2000);
    }//******** dataFile Display ********
 }

 //Voltage current function
 void VCFunction(){
 //Voltmeter1
    for(i=0;i<100;i++){
       Total+=analogRead(Voltmeter1)*Ratio1V;
       delay(2);
    }VPanel1=Total/100;
    Total=0;
 //Voltmeter2
    for(i=0;i<100;i++){
       Total+=analogRead(Voltmeter2)*Ratio2V;
       delay(2);
    }VPanel2=Total/100;
    Total=0;
 //Voltmeter3
    for(i=0;i<100;i++){
       Total+=analogRead(Voltmeter3)*Ratio3V;
       delay(2);
    }VPanel3=Total/100;
    Total=0;    digitalWrite(CVMode,HIGH);   delay(2000);
 //Ammeter1
    for(i=0;i<100;i++){
       Voltage = (analogRead(Ammeter1) / 1024.0) * 5000;
       v2 =Voltage - 2502;
       if(v2<0)
          v2=0;
       Total+=v2/66;
       delay(2);
    }CPanel1=Total/100*Ratio1C;
    Total=0;
    Voltage=0;
```

```
 //Ammeter2
    for(i=0;i<100;i++){
       Voltage = (analogRead(Ammeter2) / 1024.0) * 5000;
       v2 =Voltage - 2502;
       if(v2<0)
          v2=0;
       Total+=v2/66;
       delay(2);
    }CPanel2=Total/100*Ratio2C;
    Total=0;
    Voltage=0;
 //Ammeter3
    for(i=0;i<100;i++){
       Voltage = (analogRead(Ammeter3) / 1024.0) * 5000;
       v2 =Voltage - 2502;
       if(v2<0)
          v2=0;
       Total+=v2/66;
       delay(2);
    }CPanel3=Total/100*Ratio3C;
    Total=0;
    Voltage=0;
    delay(4000);
    if(sClr!=3)
       lcd.clear();
    sClr=3;
    Time();
    lcd.setCursor(0, 1);
    lcd.print("*P1: ");   lcd.print(VPanel1,2);   lcd.print('V');
    lcd.setCursor(14, 1);
    lcd.print(CPanel1,2);   lcd.print('A');
    lcd.setCursor(0, 2);
    lcd.print("*P2: ");   lcd.print(VPanel2,2);   lcd.print('V');
    lcd.setCursor(14, 2);
    lcd.print(CPanel2,2);   lcd.print('A');
    lcd.setCursor(0, 3);
    lcd.print("*P3: ");   lcd.print(VPanel3,2);   lcd.print('V');
    lcd.setCursor(14, 3);
    lcd.print(CPanel3,2);   lcd.print('A');
 }//Voltage current function
 void Time(){
    RTC.read(tm);
    lcd.setCursor(1, 0);
    lcd.print(tm.Hour);   lcd.print(':');   lcd.print(tm.Minute);
lcd.print(':');
    lcd.print(tm.Second);   lcd.setCursor(10, 0);
    lcd.print(tm.Day);   lcd.print('/');   lcd.print(tm.Month);
lcd.print('/');
    lcd.print(tmYearToCalendar(tm.Year));
 }
```

Appendix 2: Panel holder stand

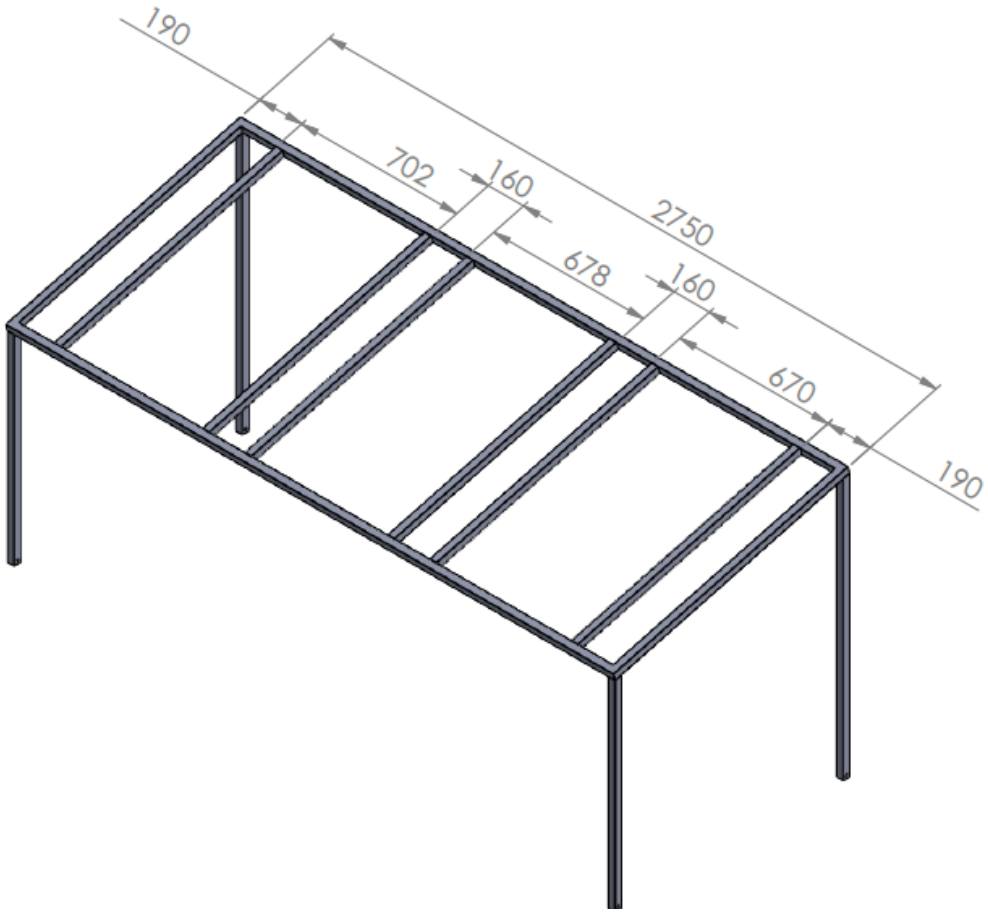

Appendix 3: Bottom panel stand

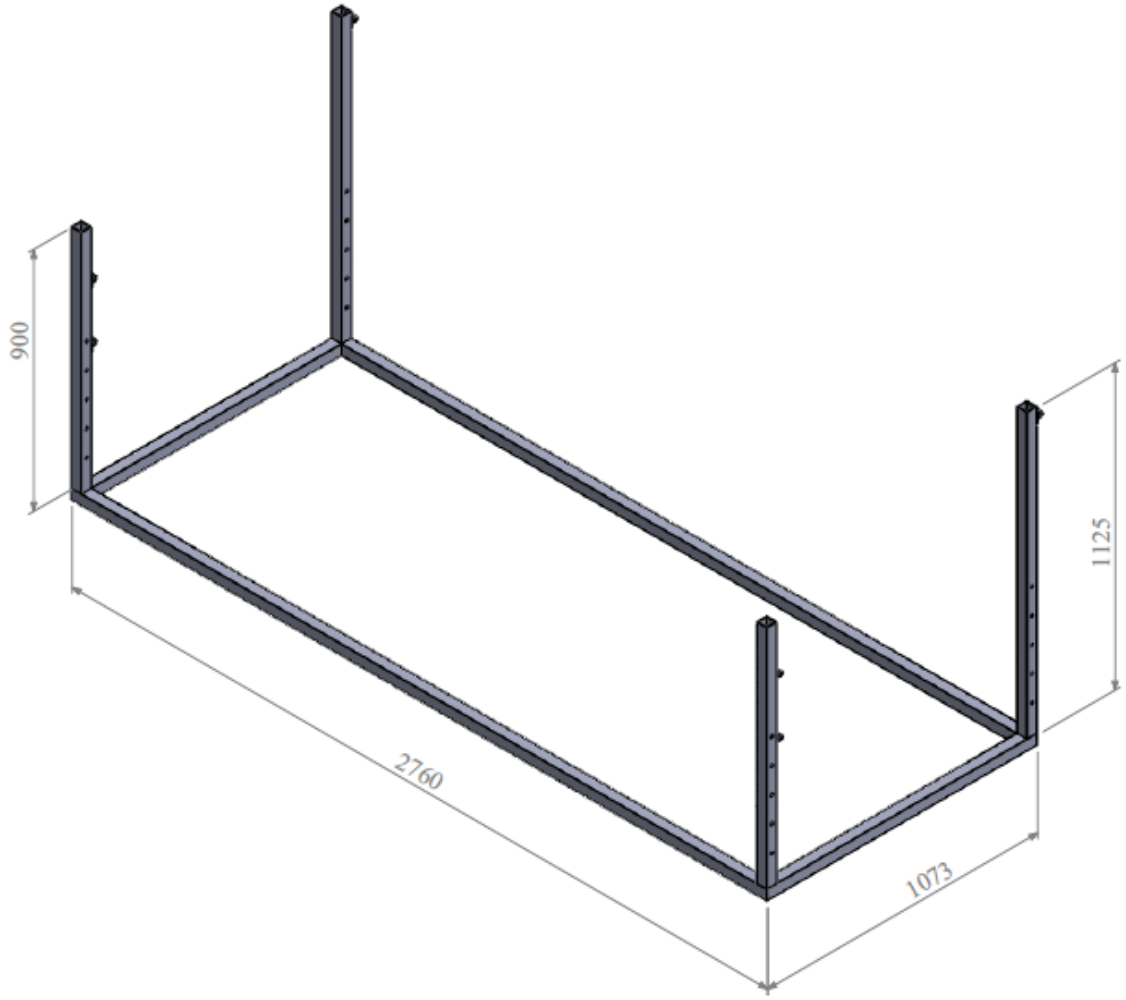

Appendix 4: Corrugated metal sheet roof holder

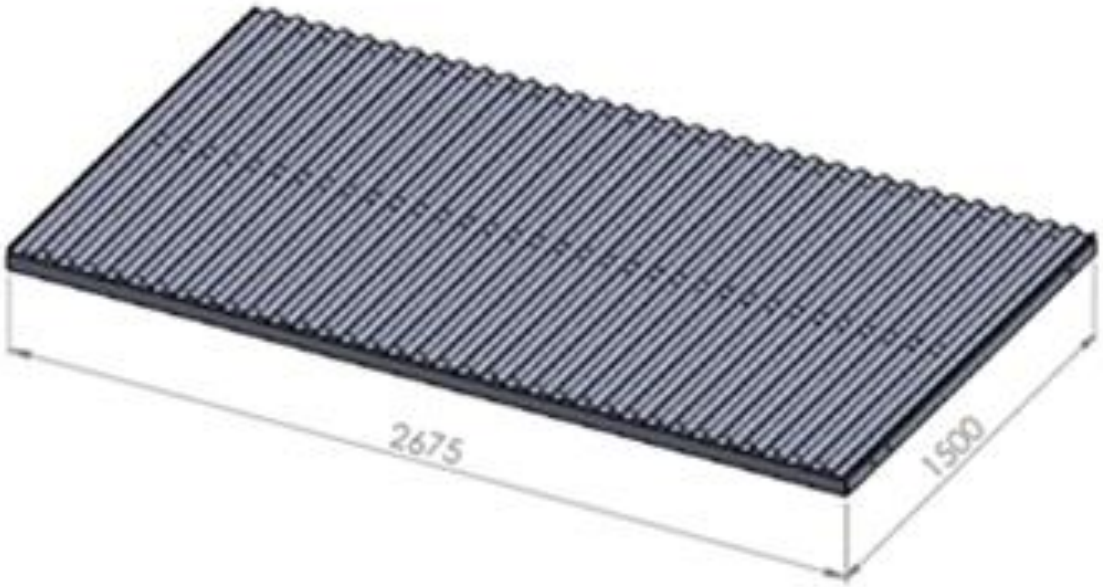

Appendix 5: Experimental mounting structure

Appendix 6: Code function for I-V curve

```
function Io=simu(Vo,G,Ta_C)
k = 1.38e-23;               %% Boltzman's constant
q = 1.602e-19;              %% electronic charge
n=1.3;                      %% ideal factor
Eg = 1.12;                  %% cell band energy gap
NCs=36;                     %% number of cells
To=273+25;                  %% Temperature at STC
Voc_To=21.6/NCs;           %% open circuit voltage at STC
Isc_To=6.3;                 %% short circuit current at STC
Tw=273+75;                  %% absolute temperature
Voc_Tw = 18 /NCs;           %% open circuit voltage at absolute
Isc_Tw=5.6;                %% short circuit current at absolute
Ta_K=273+Ta_C;              %% working cell temperature
K_cc=(Isc_Tw-Isc_To)/(Tw-To);    %% cells' short circuit current
temperature coefficient
Ipv_To = Isc_To * G;             %% photo current at STC temperature
Ipv = Ipv_To + K_cc*(Ta_K - To);  %% photo current at absolute
temperature
Id_To=Isc_To/(exp(q*Voc_To/(n*k*To))-1); %% diode current at STC
Id= Id_To*(Ta_K/To).^(3/n).*exp(-q*Eg/(n*k).*((1./Ta_K)-(1/To))); %%
diode current at absolute temperature
Xv = Id_To*q/(n*k*To) * exp(q*Voc_To/(n*k*To)); %% leakage reactance
dVdI_Voc = - 1.15/NCs / 2;   %%
Rs = - dVdI_Voc - 1/Xv;      %% series resistance
Vt_Ta = n * k * Ta_K / q;    %% thermal voltage
Vc=Vo/NCs;                   %% cell voltage
Io = zeros(size(Vc));        %% cell output current

for i=1:5;
Io = Io - (Ipv -Io - Id.*( exp((Vc+Io.*Rs)./Vt_Ta) -1))./(-1-
(Id.*(exp((Vc+Io.*Rs)./Vt_Ta) -1)).*Rs./Vt_Ta); %% absolute output current

end

end
```

Appendix 7: Command code for solar irradiance

```
clear all
clc
j=1;
for G=0.25:0.25:1

for Vo= 1:1:25

    Ta_C=25;
    Io(j, Vo)=simu(Vo,G,Ta_C);

end
j=j+1;
end
Vo=1:1:25;
figure
plot(Vo,Io)
xlim([1 25])
ylim([0 6.5])

xlabel('Output Module Voltage (V)')
ylabel('Output Module Current (A)')
```

OUTPUTS

Output 1: Acceptance letter for paper publication

DEAR DR. NICKSON JOHN,

Thank you for your contribution in our journal. At the same time we gladly inform you that your submitted manuscript (with some required revisions), for which you are the correspondence author, has been passed through our initial screening stage and is accepted for further publication process in JMEST.

As a result, your following article will be published in the **Volume. 6, Issue. 3, March – 2019 of JMEST** according to the further review process & priorities.

Your Paper will be published in online version, and all Soft Copies of certificates will be sent, you have to finish below **simple 3 Step registration process.**

Your Manuscript details are as follow:

Paper Title: EFFECT OF CORRUGATED METAL SHEET ROOF TEMPERATURE ON PERFORMANCE OF OUTDOOR MOUNTED POLYCRYSTALLINE SILICON SOLAR PV MODULE

Paper ID: JMESTN42352873

Last Date for Registration/Payment: 25-March-2019

Step - 1 : -

The paper requires editorial revisions in order to make it more understandable.

- Please use our Paper Template form.

Paper Template

Step - 2 : -

You have to make onetime payment of processing charge (USD **$45**, per article) as final step of publishing your paper at Journal.

Publication Charge includes,

- All Authors Registration charges to publish one article,
- Individual colour soft copies of Certificate of Publication to **all authors of paper**
- Paper Publication charges (Online)
- Indexing of Article
- Lifetime Preservation of Article (Open Access)

Make secured online payment directly with Credit/Debit Cards (All Master/Visa/American Express) by using below link,

http://www.jmest.org/processing-charges/

Step - 3:-

After making payment, please download Copy Right Agreement form, print it, fill it, scan it and upload it at below link **along with Final Version of paper in DOC/DOCX** format and Payment receipt if any,

Download Copyright Agreement Form

Upload Copyright Form, Final Version of Paper, Payment receipt (if any),

CLICK HERE TO UPLOAD FORMS

Kind Regards,

Editor-in-Chief

JMEST

Berlin Germany

Output 2: Research poster

PERFORMANCE ANALYSIS OF STANDALONE SOLAR PV PANEL: A CASE STUDY OF ARUSHA, TANZANIA

Nickson John, Tatiana Pogrebnaya and Thomas Kivevele

Department of Materials and Energy Science and Engineering, Nelson Mandela African Institution of Science and Technology, P. O. Box 447, Arusha, Tanzania

Email: johnn@nm-aist.ac.tz, tatiana.pogrebnaya@nm-aist.ac.tz, thomas.kivevele@nm-aist.ac.tz

Introduction

- Energy is among essential factors for social, economic and industrial development.
- Solar energy is one of the paramount renewable energy resources for rural electrification
- Sunlight reaching our environment can be rehabilitated into electricity directly by PV cell technology
- The performance of solar PV is directly proportional to the irradiance reaching the cell , and also is influenced by excessive cell temperature
- The increase in PV's temperature lowers the efficiency of PV
- Most roof installed PVs are done on the pitched roof whilst gaps and tilt angle are not carefully experimented as depicted in Figure 1.

Figure 1: Solar PVs mounted with different PV-roof spacing

Objective

The main objective of this study was to carry out experimental and theoretical performance analysis of standalone solar PV panels (polycrystalline) from three different manufacturers: A case study in Arusha, Tanzania.

Methodology

Experiments were set to present real life of outdoor roof mounted solar panel as portrayed in Figure 2.

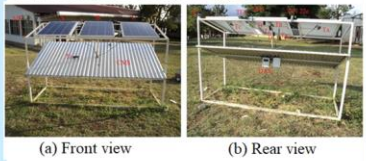

(a) Front view (b) Rear view

Figure 2: Experimental setup: Three panels A, B, and C mounted on congugated metal sheet (CMS) surface

Experimental Measurements

- ✓ Energy collector surface of solar PVs was cleaned to remove any dusts contaminated before starting the experiments.
- ✓ The experiments were conducted from 27th August 2018 to 18th of November 2018 commencing at hours with clear sky.
- ✓ Gaps variations were done manually.

The following measurements were monitored:

- Irradiance variation during the test days
- Impact of corrugated metal sheet on PV panel performance
- Effect of variance in gap on PV performance
- Solar PV panel Matlab simulation
- Effect of partial shading on solar PV panels

Results

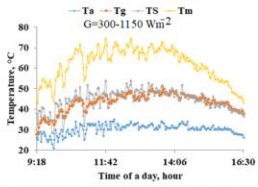

Figure 3: Variations of temperatures versus time of a day

- The PVs experienced a temperature of 60 to 74.5 °C, between 10:30 to 15:00 hours which was above the nominal operating cell temperature

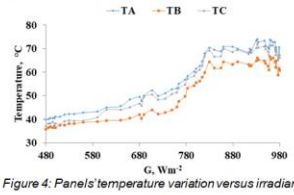

Figure 4: Panels' temperature variation versus irradiance

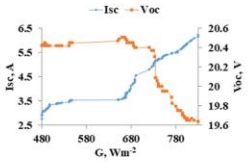

Figure 5: Short circuit current and open circuit voltage versus irradiance

- For rise in panel's temp. with increasing irradiance there was a slight drop in Voc but Isc increased.

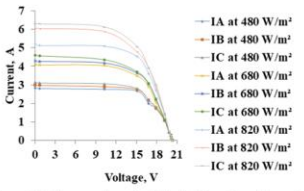

Figure 6: I-V curves for solar PVs at different irradiance for h = 0

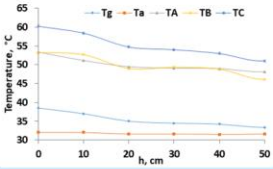

Figure 7: Temperature variation depending on gap alteration from h=0 to h=50 cm at G=820±10 Wm-2

- Temperature of the panels and the gap decreased with gap enlarged

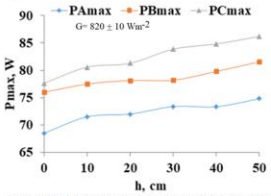

Figure 8: PVs' maximum power performance during gap alteration

- Maximum power increased after every gap enlarged

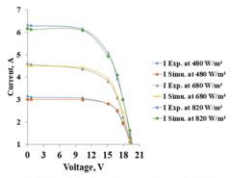

Figure 9: Simulated and experimental I-V curves

- Simulated and experimental I-V curves are found to be in good agreement

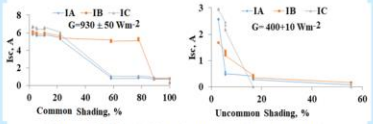

Figure 10: Effect of shading on short circuit current

- Short circuit current and open circuit voltage decreased after applying shading.
- They decreased abruptly for uncommon shade whilst for common shading abrupt decrease started at 58% of shade.

Conclusion

- Most of the faced challenges were fluctuations of outdoor readout parameters which also are the real situations that the panels face when are outdoor mounted.
- Experimental performance was carried out at irradiance of 480±10 Wm^{-2}, 680± 10 Wm^{-2}, and 820±10 Wm^{-2}, whilst the gap between the panel and CMS was varied from 0 to 50 cm.
- The power outputs were reduced by ~11% when the solar PV panel was mounted directly on the roof compared to 50 cm gap. PV extra heat originated from roof vicinity. A gap between the roof surface and panel was helpful to reduce extra heating solar panel and increase the power; the large size of the gap favored better performance of solar PV panel.
- Insignificant difference between experimental and simulated I-V curves. In general, a very good agreement is verified between the two results hence validating the findings.
- Uniform shading (pole, house or bird droppings depending on coverage on panels) could bring your system with less or no power generated. The opaque shading (front touched) stopped to generate current even when it was shaded only 11 % at the center.